The role of ColRS two-component regulatory system in rhizosphere colonization and tolerance to abiotic stress in *Pseudomonas aeruginosa*

by

Yue Zhang

B.Sc., The University of British Columbia, 2018

A THESIS SUBMITTED IN PARTIAL FULFILLMENT OF
THE REQUIREMENTS FOR THE DEGREE OF
MASTER OF SCIENCE
in
THE FACULTY OF GRADUATE AND POSTDOCTORAL STUDIES
(Microbiology and Immunology)

THE UNIVERSITY OF BRITISH COLUMBIA
(Vancouver)

April 2021

The following individuals certify that they have read, and recommend to the Faculty of Graduate and Postdoctoral Studies for acceptance, the thesis entitled:

The role of ColRS two-component regulatory system in rhizosphere colonization and tolerance to abiotic stress in *Pseudomonas aeruginosa*

submitted by Yue Zhang in partial fulfillment of the requirements

the degree of Master of Science

in Microbiology and Immunology

Examining Committee:

Cara H. Haney, Assistant Professor, Department of Microbiology and Immunology
Supervisor

Carolina Tropini, Assistant Professor, Department of Microbiology and Immunology
Supervisory Committee Member

James W. Kronstad, Professor, Department of Microbiology and Immunology
Additional Examiner

Additional Supervisory Committee Members:

Robert E. W. Hancock, Professor, Department of Microbiology and Immunology
Supervisory Committee Member

Abstract

Pseudomonas aeruginosa is a versatile bacterium found ubiquitously in the environment and is an opportunistic pathogen of diverse organisms, including animals and plants. A key determinant of bacterial adaptability is the ability to sense and respond appropriately to environmental stimuli. ColRS is a two-component regulatory system previously shown to be required for *P. fluorescens* colonization of plant roots (the "rhizosphere") and *P. aeruginosa* virulence in *C. elegans*; however, the mechanisms by which ColRS regulates fitness in a host environment are unknown. I found that *colR* and *colS* deletion mutants in *P. aeruginosa* were significantly impaired in their ability to colonize the rhizosphere of Arabidopsis. In addition, we showed that *colR* in the *P. aeruginosa* cystic fibrosis epidemic isolate, LESB58, is required for virulence in a mouse abscess model. Using RNA-seq, I found a total of 128 genes that were dysregulated in the *colR* mutant in the rhizosphere, many of which have products that are predicted to localize to the cytoplasmic or outer membranes, suggesting ColRS may function in maintaining membrane integrity. Using *P. aeruginosa* transposon insertion mutants in *colR*-dependent genes, I identified novel genes required for rhizosphere colonization, including the protein tyrosine phosphatase *tpbA*, diacylglycerol kinase *dgkA*, and a type 2 phosphatidic acid phosphatase. Lastly, I showed that *P. aeruginosa colR* is required for tolerance to high levels of iron, zinc, and manganese, and for growth at acidic pH. Because functional analysis of rhizosphere gene expression showed that high iron concentration and low pH are stresses that may be present in the rhizosphere, the ColRS two-component system likely promotes *P. aeruginosa* colonization of the Arabidopsis rhizosphere through regulation of genes required to protect against these stresses.

Lay Summary

The ability to sense and respond to environmental stimuli is important for bacterial versatility, including the ability of bacteria such as *Pseudomonas aeruginosa* to colonize and cause disease in both plants and animals. To adapt to new environments, bacteria have signaling pathways to sense environmental stimuli and respond by altering gene expression. In this study, I characterized a signaling pathway in *P. aeruginosa*, and found that it is required for the bacterium to colonize plant roots and to cause disease in mice. I found that loss of this signaling pathway may alter composition of the bacterial membranes, which protect the bacteria from their external environment. I show that this signaling pathway is important for protection against low pH and heavy metal toxicity, which may be important for host association.

Preface

The work in this thesis was conducted under the supervision of Dr. Cara H. Haney. The thesis was written entirely by me, and all experiments and data described were performed and analyzed by me with the following exceptions. Mouse experiments were conducted by Morgan Alford and Daniel Pletzer, under the supervision of Dr. Robert E. W. Hancock. Data in Figure 3 were provided by Daniel Pletzer and Morgan Alford. Chapter 2.1.5 and 2.1.6 describing the methodology of the mouse experiments were written by Morgan Alford and edited by me.

Table of Contents

List of Tables

List of Figures

List of Symbols

α	alpha
Δ	delta
μ	micron
°	degrees

List of Abbreviations

ATP: Adenosine triphosphate

Cb: Carbenicillin

c-di-GMP: Bis-(3′-5′)-cyclic dimeric guanosine monophosphate

cDNA: complementary deoxyribonucleic acid

CF: Cystic fibrosis

CFU: Colony forming units

GFP: Green fluorescent protein

Gm: Gentamicin

L-Ara4N: 4-Amino-L-arabinose

L-gln: L-glutamine

LB: Lysogeny broth

LPS: Lipopolysaccharides

MS medium: Murashige and Skoog medium

OD_{600}: Optical density at 600 nm

PAP2: Type 2 phosphatidic acid phosphatase

PCR: Polymerase chain reaction

pEtN: Phosphoethanolamine

PTI: Pattern-triggered immunity

qRT-PCR: Quantitative reverse transcriptase polymerase chain reaction

spp: Species

T6SS: Type 6 secretion system

Acknowledgements

I would like to extend my gratitude to the staff and facilities at the University of British Columbia, and my funding sources, for providing me the opportunities and the resources to carry out my research. I am extremely grateful for my supervisor and mentor, Dr. Cara H. Haney, whose patience, compassion, and excitement for science made my time in graduate studies an enriching experience. I would also like to sincerely thank my committee members, Dr. Robert E. Hancock and Dr. Carolina Tropini, for taking their time to give me constructive feedback and providing their valuable perspectives and insights on my project.

I am grateful to have had amazing lab mates in the Haney, Hancock, and Kronstad labs that have helped me in various ways throughout my degree. I especially want to thank Christina Wiesmann, who has been both a great project partner and an amazing friend. I hope we can continue to go on skiing and hiking trips in the future. I would also like to thank Nicole Wang for introducing me to many new opportunities, and Yang Liu for her ever-present cheeriness in the lab. I would like to credit Morgan Alford and Daniel Pletzer, who have been amazing collaborators that were always willing to help and answer my questions, and without whom the mice experiments would not have been possible. To the Kronstad lab friends I made in the during my final year, thank you for the outdoors adventures and online game nights during this pandemic.

Lastly, I owe my family a debt of gratitude. They have provided me with unwavering moral and financial support throughout my education and beyond.

Chapter 1: Introduction

1.1 Modeling *Pseudomonas aeruginosa* pathogenesis.

Bacterial ESKAPE pathogens have a high level of antibiotic resistance and a high frequency of multidrug-resistant variants (1). ESKAPE pathogens [*Enterococcus faecium, Staphylococcus aureus, Klebsiella pneumoniae, Acinetobacter baumannii, Pseudomonas aeruginosa*, and *Enterobacter* species (spp.)] include some of the leading causes of nosocomial infections globally (1, 2). The increasing prevalence of multidrug resistant pathogens in hospitals urgently requires the development of alternative therapies (2).

P. aeruginosa is a Gram-negative Gammaproteobacterium ESKAPE pathogen, which is notoriously difficult to treat. *P. aeruginosa* is an opportunistic human pathogen, which is normally harmless to healthy individuals, but can cause serious disease including septicemia in severe burn patients, chronic wound infections such as in leg ulcers, and untreatable infections in the lungs of individuals with the genetic disorder cystic fibrosis (CF) (3–5). *P. aeruginosa* infections usually occur in biofilms, which are associated with high resistance to antimicrobial compounds due to chemical properties of the extracellular matrix, and altered metabolic and physiologic characteristics of cells within biofilms (6, 7). *P. aeruginosa* is also intrinsically resistant to many environmental toxins due to its low outer membrane permeability, abundance of efflux pumps, and the ability to develop adaptive resistance to antibiotics (8).

P. aeruginosa has a remarkable host range and is an opportunistic pathogen of not only humans, but rodents, plants, nematodes, fish, and insects, allowing the flexibility of studying *P. aeruginosa* in many different infection and colonization models (7, 9–13). A reason for the success of *P. aeruginosa* as an opportunist is its adaptability and metabolic versatility (14). *P.*

aeruginosa is found ubiquitously on surfaces, in soil and in aquatic environments, and is commonly found associated with the organisms that inhabit those environments (15).

Mammalian model systems such as mice are commonly used for the study of human pathogens such as *P. aeruginosa* because of their physiological similarity to humans. The mouse thermal injury or burn model examines acute *P. aeruginosa* virulence, and involves subjecting mice to non-lethal thermal injury before subcutaneous injection of *P. aeruginosa* into the burn wounds (9). Rodent models have also been developed to mimic the nature of chronic *P. aeruginosa* infections. In a rat lung chronic infection model, *P. aeruginosa* cultures are embedded in alginate beads and surgically inserted into the rat lung, establishing a local infection that is not rapidly cleared by the immune system due to the presence of the alginate matrix (16). A murine subcutaneous abscess chronic infection model was recently developed by Pletzer *et al.* for the study of Gram-negative bacterial pathogens including *P. aeruginosa* (17). This model was used in this study and further discussed in Chapter 2. Suspensions of *P. aeruginosa* strain LESB58, a Liverpool cystic fibrosis epidemic isolate (18), injected into the thin skeletal muscles on the backs of shaved mice establish localized infections in abscesses that can be easily monitored over the course of the infection (17). While mammalian infection models are undoubtedly valuable tools to elucidate host and bacterial factors relevant to human infections, these models are often not easily accessible, technically challenging to use, and costly to maintain.

Many non-mammalian hosts have also been used to study *P. aeruginosa* virulence and host responses, such as the nematode *Caenorhabditis elegans*, the insects *Drosophila melanogaster* and *Galleria mellonella*, zebrafish, and plants including Arabidopsis, sweet basil and poplar trees (11–13, 19–21). The appeal of using non-mammalian hosts comes from reduced

space, cost, and time efficiency for rearing, reduced ethical concerns, increased tractability, and increased availability of high throughput screening. Findings in non-mammalian hosts can be retested in vertebrate models, such as the rodent models described above (7, 20, 22, 23). These multi-host studies were used to more efficiently screen and investigate the molecular and genetic mechanisms of bacterial pathogenesis (22).

1.2 Multi-host studies of *P. aeruginosa* pathogenesis.

Early studies using nematodes, insects, and plants to study bacterial pathogenesis have found that, despite the vastly different physiology of plants and animals, bacteria can employ an overlapping set of virulence factors across these hosts (20, 22, 24). For example, a high throughput screen of *P. aeruginosa* mutants in a slow killing assay in *C. elegans* identified a chemotaxis-related gene *cheB2* that was required for virulence in both *C. elegans* and a mouse lung infection model (23). *P. aeruginosa* mutants lacking an endotoxin *toxA*, a phospholipase *plcS* (also known as *plcH*), and a global response regulator *gacA*, had reduced virulence in both an Arabidopsis leaf infection model and a mouse full-thickness skin thermal burn model (24). These studies indicate that virulence factors in broad host-range mammalian pathogens can be effectively identified using non-vertebrates such as nematodes, insects, and plants.

The model nematode *C. elegans* has been widely used to study innate immunity and bacterial pathogenesis. *C. elegans* are natural bacterivores, but accumulation of pathogenic bacteria such as *P. aeruginosa* in their gut can lead to infection and death (25). Using *C. elegans*, a study demonstrated the importance of mitochondrial turnover, or mitophagy, in *P. aeruginosa* infection (26). The authors found that the *P. aeruginosa* siderophore, pyoverdine, induced hypoxic responses in *C. elegans* through iron sequestering, causing extensive fragmentation of

mitochondria. Loss of mitophagy in *C. elegans* promoted increased killing by *P. aeruginosa*, demonstrating the importance of this process in defense against the pathogen. Mitophagy was shown to alleviate the stress of iron depletion in mammalian cells as well, suggesting that mitophagy is a conserved defense mechanism against the siderophores of *P. aeruginosa* (26).

The insect *G. mellonella* has also been used to study *P. aeruginosa* virulence. *G. mellonella* larvae are highly susceptible to systemic infection by *P. aeruginosa*. Infection of *G. mellonella* with just 10 *P. aeruginosa* cells was able to cause 100% mortality in the insect larvae within 24 hours (27). A positive correlation was found between *P. aeruginosa* virulence in *G. mellonella* and virulence in a mouse burn model (20). *P. aeruginosa* mutants that had increased median lethal dose (LD50) in *G. mellonella* generally also resulted in decreased mice mortality in the mouse burn model (20). *G. mellonella* has also been used to model the efficacy of *in vivo* phage therapy against *P. aeruginosa* infection (28, 29). Given the high prevalence of antibiotic resistant *P. aeruginosa* in clinical settings, phage therapy is an attractive alternative course of treatment (28). *In vivo* efficacy of two novel bacteriophages with *in vitro* activity against extensively drug resistant (XDR) *P. aeruginosa* were tested using both *G. mellonella* and a mouse acute pneumonia model (29). Phage treatment resulted in greater than 50% increase in rates of *G. mellonella* survival, and greater than 66% increase in rates of mouse survival (29). These studies suggest that *G. mellonella* could be used to model both virulence of and treatment efficacy against *P. aeruginosa* infections in mammals.

Both leaf and root infection models of plants are used to study *P. aeruginosa* pathogenesis (11, 24, 30). Arabidopsis is a commonly-used model plant that is genetically tractable, has a short generation time, and a small sequenced genome (31). Conservation of *P. aeruginosa* virulence genes across plants and animals was shown by Rahme *et al*. In this study,

the authors screened 2500 *P. aeruginosa* transposon mutants and identified 9 mutants that elicited decreased disease symptoms in lettuce and Arabidopsis leaves. All 9 mutants also resulted in decreased mortality when injected into the mouse full-thickness skin thermal burn model (32). *P. aeruginosa* also colonizes the plant rhizosphere and can infect plants through their roots. A study of *P. aeruginosa* infection of poplar tree roots found upregulation of many *P. aeruginosa* virulence factors including genes encoding hemolysin and a hemolysin regulator, which had not been previously studied (21). Inactivation of the hemolysin gene significantly reduced both *P. aeruginosa* pathogenesis and colonization of the poplar tree, and exhibited decreased cytotoxicity towards red blood cells (21). Collectively, the use of non-vertebrates has provided valuable insight into the mechanisms of bacterial pathogenesis and host-microbe interactions.

1.3 Plants are natural hosts of *P. aeruginosa.*

Soils and plants are natural habitats and reservoirs of *P. aeruginosa* (33). *P. aeruginosa* strains have been isolated from healthy ornamental plants, and vegetable foods in hospitals, which may be sources of *P. aeruginosa* nosocomial infections (34, 35). *P. aeruginosa* robustly colonizes the rhizosphere, the environment on and in close proximity to plant roots (36, 37). Though the reference *P. aeruginosa* strain PAO1 was isolated from a human would infection, it can colonize the wheat rhizosphere even in natural soil with the presence of other microorganisms (38). PAO1 can grow as well as the biocontrol bacterium *P. fluorescens* F113 in the rhizosphere of wheat and sugar beet, making PAO1 a good strain for modeling *P. aeruginosa*-plant interactions in the rhizosphere (38, 39)

1.3.1 *P. aeruginosa* as a plant pathogen.

P. aeruginosa is a natural opportunistic phytopathogen. A study from 1942 identified *P. aeruginosa* as the etiological agent of a prevalent tobacco disease in the Philippines (40). *P. aeruginosa* exhibits greater phytopathogenicity in warm temperature and high humidity, which are favourable conditions for its growth. The Arabidopsis leaf infection model uses these conditions to study *P. aeruginosa* virulence. Plants infected with *P. aeruginosa* were incubated at near 30˚C with above 70% humidity, after which *P. aeruginosa* caused disease symptoms and grew in the leaf tissue to numbers comparable to the well-studied plant pathogen, *P. syringae* (24). At lower temperature and humidity, *P. aeruginosa* growth in leaf tissue is low and variable and causes attenuated disease symptoms, consistent with its role as an opportunistic pathogen of plants (41).

P. aeruginosa can cause disease in plants when inoculated into the rhizosphere (11, 21, 30). Inoculation of *P. aeruginosa* into the rhizosphere of both Arabidopsis and sweet basil caused disease symptoms including black necrotic lesions on the roots and water soaked lesions on leaves, resulting in plant mortality (11). Both PAO1 and PA14 form biofilm-like communities on the root surfaces of Arabidopsis and sweet basil, when viewed using scanning electron and phase contrast microscopy. *P. aeruginosa* inoculation into the rhizosphere of poplar trees caused wilting and mortality (21). The same study found that *P. aeruginosa* virulence reduced the germination rate of barley seeds (21). *P. aeruginosa* infection of canola seedlings reduced canola root and shoot mass, and induced the development of black spotting on leaves (30). These studies showcase the versatility of *P. aeruginosa* as a general plant pathogen.

1.3.2 *P. aeruginosa* as a biocontrol agent against other plant pathogens.

Besides exhibiting virulence against its plant or animal hosts, *P. aeruginosa* also secretes toxins that have antimicrobial activity against other species of bacteria or fungi, making them strong competitors. Because of their ability to outcompete other microorganisms, *P. aeruginosa* strains can act as biocontrol agents that protect agriculturally important plants against diseases caused by other plant pathogens (36, 37, 42). *P. aeruginosa* PNA1, isolated from the chickpea rhizosphere in India, can protect pigeonpea and chickpea against the fungal disease Fusarium wilt (36). *P. aeruginosa* BR3p was isolated from rice roots and can protect rice from bacterial leaf blight caused by *Xanthomonas oryzae* pv. *oryzae* (37). The protective natures of PNA1 and BR3p were likely due to production of siderophores and toxic secondary metabolites including pyocyanin, phenazine antibiotics, rhamnolipids, and 4-hydroxy-2-alkylquinolines (36, 37). Though *P. aeruginosa* can protect plants against agricultural pathogens, there is limited traction for the use of *P. aeruginosa* as a biocontrol agent in the field due to its potential to act as a plant and human pathogen (37). Regardless of whether *P. aeruginosa* is acting as a pathogen or as a biocontrol agent, it is evident from these studies that strains of *P. aeruginosa* are genetically well-equipped to grow in association with plant hosts.

1.4 *Pseudomonas* mechanisms required to colonize the plant rhizosphere.

As inhabitants of soil, *P. aeruginosa* and other bacteria naturally encounter plant roots and the plant rhizosphere. The rhizosphere is rich in carbon compounds secreted by the plant, called root exudates. Root exudates contain soluble, low molecular weight compounds that are released by the roots passively or actively into the soil, and are the major sources of organic carbon in the soil (43). These include primary metabolites such as sugars, amino acids, organic

acids, and secondary metabolites such as aromatic compounds. The composition and functions of root exudate components have been extensively studied and reviewed (44–46). Though root exudates represent a significant carbon sink for the plant, root exudates provide organic nutrients to support the rhizosphere microbiome, and antimicrobial compounds to defend against phytopathogens (44). These plant-secreted organic compounds support the growth of approximately 10^2 to 10^5 times more microorganisms than bulk soil (44).

To survive in the rhizosphere, microbes must utilize rhizosphere nutrients and evade or protect themselves against plant antimicrobial compounds. Because *Pseudomonas* are effective rhizosphere colonizers, use of *Pseudomonas* strains has facilitated identification of mechanisms required for rhizosphere colonization. Use of transposon insertion mutants in *P. fluorescens* WCS365 identified genes required for rhizosphere fitness that affect motility, chemotaxis, carbon metabolism, amino acid biosynthesis, and lipopolysaccharide (LPS) modification (47–50). More recently, use of high-throughput genome-wide screens such as transposon mutagenesis combined with next-generation sequencing (TnSeq) have identified bacterial genes that are important for rhizosphere colonization and interactions with the plant. TnSeq screens in *P. simiae* WCS417 and *P. fluorescens* WCS365 identified genes that positively or negatively affect bacterial fitness in the rhizosphere (51, 52).

A genome-wide TnSeq screen of *P. simiae* WCS417 identified genes that positively contribute to fitness in the rhizosphere. Rhizosphere fitness determinants included genes whose products affect cell motility, biogenesis of the cell wall or envelop, and carbohydrate transport and metabolism. Mutants in genes with outer membrane-associated functions, including a gene that encodes an outer membrane protein from the OmpA family, and genes in the *arn* operon, encoding proteins responsible for the addition of 4-Amino-l-arabinose (L-Ara4N) to lipid A of

LPS, were depleted in the rhizosphere (51), suggesting the importance of outer membrane functions in rhizosphere adaptation. TnSeq was used similarly in WCS365, to identify bacterial genes that not only were important in fitness during rhizosphere colonization but likely function to evade plant defenses (52). Liu *et al*. screened for mutants with decreased fitness in wildtype Arabidopsis but had no effect on or had increased fitness in an immunocompromised Arabidopsis *dde2*/*ein2*/*pad4*/*sid2* quadruple mutant (*deps*) impaired in immune hormone signaling. Among the genes identified were *morA*, encoding a c-di-GMP phosphodiesterase and *spuC,* encoding a putrescine aminotransferase, which contribute to bacterial evasion of plant pattern-triggered immunity (PTI), possibly through modulation of polysaccharide production and biofilm formation (52). Collectively, these studies have contributed to the growing body of knowledge on the molecular mechanisms of rhizosphere colonization and plant-bacterial interactions.

1.5 The bacterial two-component system ColRS is required for fitness in the rhizosphere.

In multiple forward genetic screens described above, *colRS* encoding a two-component regulatory system, was consistently required for fitness in the rhizosphere (50–52). This two-component system was first identified by testing single *P. fluorescens* WCS365 transposon insertion mutants for competitive defects in rhizosphere colonization. A transposon insertion mutant in *colS* had a greater than 300-fold fitness defect in the potato rhizosphere (50, 53). The *colS* mutant was not impaired in many known rhizosphere colonization factors including motility, chemotaxis, growth on rich media, biosynthesis of amino acids, and production of O-antigen (50). In a TnSeq screen, *P. simiae* WCS417 *colS* was also required for rhizosphere fitness, but not required for growth in any of the tested carbon sources (51). Liu *et al*. found that

mutation in *colR* negatively impacted the fitness of WCS365 growing in the rhizosphere of both wildtype and immunocompromised Arabidopsis, which suggests that the fitness defect was not related to plant hormone-mediated immune responses. While *colRS* was repeatedly identified through forward genetic screens, why this two-component system is required for rhizosphere fitness remains unclear.

Further characterization of the WCS365 *colS* mutant found that it has altered resistance to antibiotics and altered outer membrane structure. A *colS* mutant has increased resistance to streptomycin, rifampicin, spectinomycin and tetracycline, but slightly decreased resistance to polymyxin B, which is a cationic antibiotic that interacts with the negatively charged bacterial outer membrane as part of its mechanism of killing (53, 54). The same study also found that ColRS regulates *wapQ*, encoding a heptose kinase located adjacent to the *colRS* operon predicted to phosphorylate heptoses in the LPS core (53). These results suggested that the *colS* mutant has an altered membrane permeability, possibly due to changes in LPS structure.

The outer leaflet of the outer membrane of Gram-negative bacteria is composed of LPS, and directly exposed to the external environment. Bacterial outer membranes play important roles in protection against toxic compounds, nutrient uptake, and stimulation of the host immune system (55). Consequences of altered LPS structure were seen in multiple systems of host-bacterial interactions (55). Length of the O-antigen, for example, was important for colonization of the tomato rhizosphere and for immune evasion by *P. aeruginosa* in a zebrafish infection model (56, 57). Interestingly, mutations in *colS* also impaired virulence in a *C. elegans* slow killing assay (23). Because ColRS may be a common *Pseudomonas* colonization and/or virulence factor in plants and nematodes, I hypothesized that studying the ColRS two-component

system in *P. aeruginosa* could identify genes that are required for host-association across plants and animals.

1.6 ColRS is a conserved two-component system in *Pseudomonas.*

ColRS is a two-component system, composed of the sensory histidine kinase ColS, and the response regulator ColR. Two-component systems are simple regulatory cascades commonly found in bacteria and regulate numerous processes from growth and metabolism to virulence and antibiotic resistance (58–60). The sensor kinase perceives an environmental stimulus and undergoes autophosphorylation at a histidine residue, which is subsequently transferred to an aspartate residue in the response regulator (61). The phosphorylated response regulator typically undergoes a conformational change (61). Most response regulators, including ColR, contain a helix-turn-helix DNA-binding domain and act as transcription factors that directly bind to DNA to regulate gene expression (62).

ColRS is well conserved throughout species in the *Pseudomonas* genus (http://www.pseudomonas.com, 78). BLAST local alignments of ColRS amino acid sequences revealed high sequence similarity between three distantly related *Pseudomonas* strains (Figure 1). *P. aeruginosa* PAO1 ColS has 62% identity (E value = 0.0) with *P. putida* KT2440 ColS and 61% identity (E value = 0.0) with *P. fluorescens* WCS365 ColS. PAO1 ColR has 89% identity (E value = 2e-152) with KT2440 ColR and 88% identity (E value = 2e-150) with WCS365 ColR. The phosphorylated histidine (ColS) and aspartate (ColR) residues and the DNA-binding residues in the C-terminal helix-turn-helix domain of ColR are conserved across all three strains (Figure 1). Additionally, a ExxE motif in ColS required for ColRS-dependent gene expression in

response to iron or zinc in *P. putida*, which potentially directly binds Fe^{3+} or Zn^{2+} ions, is conserved across all three strains (Figure 1; 64).

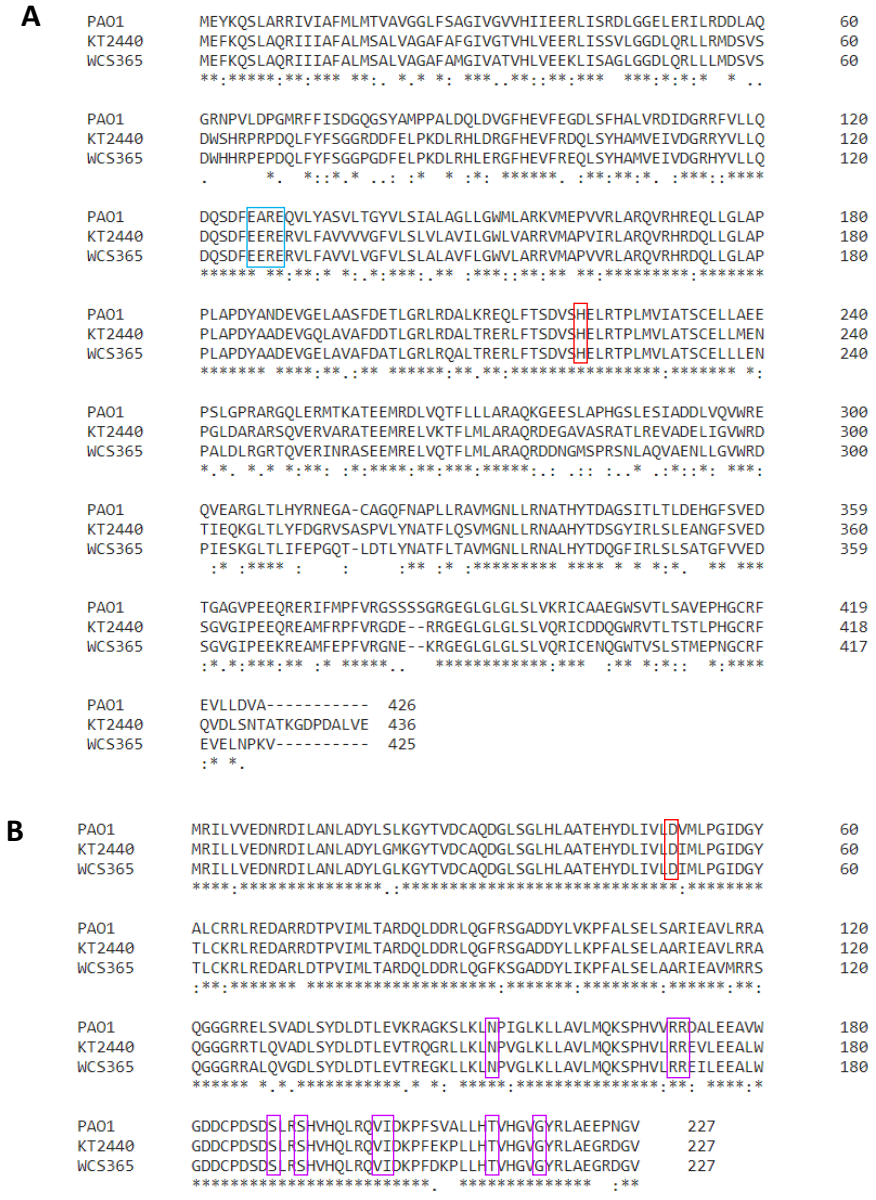

Figure 1. Multiple sequence alignment of the ColRS two-component system in different *Pseudomonas* spp. strains. (A) ColS and **(B)** ColR amino acid sequences from *P. aeruginosa* PAO1, *P. putida* KT2440, and *P. fluorescens* WCS365 were aligned using the Clustal Omega Multiple Sequence Alignment tool (https://www.ebi.ac.uk/Tools/msa/clustalo/). The blue box indicates the ExxE motif predicted to bind and sense iron and zinc (64). The red boxes indicate the conserved histidine (H) or aspartate (D) that is phosphorylated in ColS or ColR, respectively. The purple boxes indicate DNA-binding sites in ColR. Conserved residues excluding the ExxE motif were identified using Interpro. Amino acid sequences were obtained from pseudomonas.com or NCBI.

Although a *P. aeruginosa colS* mutant had reduced virulence in a high-throughput *C. elegans* screen (23), ColRS has not been extensively studied as a virulence or colonization factor in *P. aeruginosa*, and its regulon in *P. aeruginosa* is poorly characterized. Studies on ColRS in other *Pseudomonas* spp. can be used to provide further insights into the functions of this regulatory system in *P. aeruginosa.*

1.7 Loss of ColRS is associated with diverse phenotypes in *Pseudomonas.*

ColRS in *P. aeruginosa* contributes to clinical polymyxin B resistance (65). Though mutation in *colRS* in a wildtype *P. aeruginosa* background did not affect polymyxin B resistance, mutation of *colRS* abrogated polymyxin B resistance in a *phoQ* mutant (65). Clinical isolates of *P. aeruginosa* with resistance to polymyxin B often harbor mutations in *phoQ* that result in constitutive addition of L-Ara4N to lipid A (66). Covalent addition of L-Ara4N to the phosphate groups on lipid A confers resistance to polymyxin B by neutralizing negative charges on LPS thereby reducing the affinity of the outer membrane to the cationic antibiotic (67). The lipid A of the *phoQ* and *colRS* mutant still had the L-Ara4N modifications seen in the *phoQ* mutant, indicating that there may be a distinct mechanism by which *colRS* affects polymyxin B resistance (65).

In *P. putida*, mutants in *colRS* have impaired growth in *in vitro* stress conditions. ColRS is required for growth on minimal media containing phenol, which can accumulate in bacterial membranes resulting in membrane disruption and leakage of intracellular contents (68). The degree of *colR* mutant susceptibility to phenol was dependent on the carbon source in the media; use of glucose rather than citrate exacerbated the *colR* mutant growth defect on phenol (69). Deletion of *oprB1* partially alleviated the phenol susceptibility of the *colR* mutant in the presence

of glucose, presumably because glucose transport through the OprB1 outer membrane porin contributes to phenol entrance in *P. putida* (69). The authors suggested that the *colR* mutant membrane had increased intrinsic permeability to phenol through regulation of genes encoding other membrane-associated proteins, and phenol entrance through OprB1 increased the accumulation of phenol in the *colR* mutant beyond its threshold toxicity (69).

ColRS is also required for heavy metal tolerance, including zinc, manganese, cadmium, and iron tolerance in *P. putida*, and zinc tolerance in *P. aeruginosa* (64, 70). Though these transition metals are essential micronutrients, high levels can cause oxidative stress through Fenton chemistry and enzyme inhibition through mismetallation of essential metalloenzymes (71, 72). Addition of $ZnSO_4$, $FeSO_4$, $MnSO_4$, and $CdSO_4$ can activate the expression of some *colR*-dependent genes (discussed below) potentially via the conserved ExxE motif in the periplasmic region of ColS (Figure 1; 64). Addition of excess zinc induced much greater changes in the *P. putida* proteome in the a *P. putida colR* mutant compared to wildtype *P. putida*, including higher induction of alginate biosynthesis proteins, likely through activation of *colR*-independent zinc tolerance pathways (73). These results collectively suggest that ColRS regulates *Pseudomonas* membrane permeability and stress response pathways in the presence of specific abiotic stressors.

1.8 The ColRS regulon in *Pseudomonas*

Identifying ColRS-regulated genes is key to elucidating the mechanisms by which ColRS influence membrane integrity. A study in *P. putida* identified a ColR-binding consensus sequence that was used to predict several novel ColR-regulated genes (63). As expected, many ColR-regulated genes encode products involved in outer membrane modifications and membrane

lipid homeostasis. In fact, 56% of the putative ColR-binding sites in *P. putida* are upstream of genes with products that are implicated in membrane functions (63).

In *P. fluorescens*, ColR regulates the expression of an operon directly adjacent to *colRS* that consists of *orf222* and *wapQ*, encoding a predicted methyltransferase, and an LPS kinase, respectively (53). Disruption of this operon also impaired the rhizosphere fitness of *P. fluorescens* (53). Expression of the *P. putida wapQ* homolog was induced by ColR in response to phenol and high levels of iron, zinc, manganese, and cadmium (63, 64). The *P. aeruginosa* homolog of Orf222 (WarA) interacts with c-di-GMP, and together with the WapQ homolog (WarB), likely acts by methylating and phosphorylating the terminal-reducing end of a growing O-antigen chain on LPS to terminate its synthesis (57). Loss of *orf222/warA* resulted in an increase in the average length of O-antigen chains in the outer membrane and reduced virulence in both *G. mellonella* and zebrafish infection models (57). Though ColRS has not been shown to regulate *warAB* in *P. aeruginosa*, the evidence in two other *Pseudomonas* spp. and the conserved genomic context of the operon adjacent to *colRS* suggest this is likely the case in *P. aeruginosa* as well.

In addition to the methyltransferase and LPS kinase, ColR regulates the expression of other LPS modifying enzymes. In *P. putida*, ColR negatively regulates the lipid A 3-O-deacylase *pagL*, which encodes an enzyme that cleaves an acyl chain from the lipid A of LPS. *P. putida* ColR also positively regulates *cptA*, encoding a phosphoethanolamine (pEtN) transferase that likely covalently adds a pEtN group to the LPS core based on the function of its homolog in *Salmonella enterica* (63, 64). In response to zinc, ColR in *P. aeruginosa* also regulates another pEtN transferase *eptA*, which is not orthologous to *P. putida cptA* (70). EptA catalyzes the

addition of pEtN to the lipid A of LPS, and though this addition was induced in *P. aeruginosa* by zinc, it was not required for zinc tolerance (70).

ColR may also regulate the expression of genes whose products are required for metabolism of phospholipids that make up the structure of membrane bilayers. *P. putida* ColR induces the expression of *dgkA* encoding a diacylglycerol kinase, and a gene encoding a type 2 phosphatidic acid phosphatase (PAP2) (63). DgkA and PAP2 convert diacylglycerol to phosphatidic acid, or phosphatidic acid to diacylglycerol, respectively (74, 75). Both phosphatidic acid and diacylglycerol are key intermediates, and precursors to the synthesis of many major membrane phospholipids (74, 75). DgkA is also important for phosphatidylglycerol turnover, which is important for tolerance to osmotic stress in *E. coli* (75). This suggests that loss of *colR* may result in decreased membrane structural integrity through disruption of phospholipid synthesis and turnover.

1.9 Objectives

Though many genes are regulated by ColRS in *P. putida in vitro*, the ColR regulon is poorly characterized in *P. aeruginosa* and *in vivo*. While overlap of *colR*-dependent genes between *P. fluorescens, P. putida,* and *P. aeruginosa* suggests that there is some conservation in the ColR regulon between *Pseudomonas* spp., the degree of conservation is unknown. Given the potential role of ColRS in host colonization and virulence, further investigation of the genes regulated by ColRS in *P. aeruginosa in vivo* could lead to the identification of novel colonization or virulence factors in a clinically important human pathogen.

My objectives for this study were:

1. **Test whether *P. aeruginosa colR* and *colS* are required for colonization of the Arabidopsis rhizosphere and virulence in a mouse subcutaneous abscess model.**

Because there are conserved in bacterial colonization and virulence factors across plant and animal hosts, and because membrane integrity and LPS structure are important for virulence and tolerance to environmental toxins, I hypothesized that ColR and ColR-regulated genes would be required for host colonization and/or virulence in *P. aeruginosa* in both plants and animals. To test this hypothesis, I measured the growth of *colR* (PAO1 Δ*colR*) and *colS* (PAO1 Δ*colS*) clean deletion mutants in *P. aeruginosa* PAO1 in the rhizosphere of the plant Arabidopsis. PAO1 (14) was the primary wildtype *P. aeruginosa* strain used in this study, as this is a well-studied reference strain with a well-characterized genome, and can colonize the plant rhizosphere (11, 21). To test the effect of the loss of *colR* in an animal model, I generated a *colR* deletion mutant in the *P. aeruginosa* chronic infection isolate, LESB58 (18), which was tested for virulence and colonization in a mouse subcutaneous abscess model of chronic infection (17).

2. **Identify genes induced in the rhizosphere in a *colR*-dependent manner.**

Because ColR is a DNA-binding response regulator in *Pseudomonas*, I hypothesized that there would be differences in the gene expression between PAO1 and PAO1 Δ*colR* in the rhizosphere, which would include genes that are directly and indirectly regulated by ColR. Genes dysregulated in the absence of *colR* may provide insights into the mechanisms by which ColR regulates rhizosphere colonization. Next-generation sequencing of total bacterial RNA (RNA-seq) was employed to identify transcriptional differences between PAO1 and PAO1 Δ*colR* and to identify *colR*-dependent gene expression. I identified genes that were significantly differentially expressed between PAO1 or PAO1 Δ*colR* in the rhizosphere compared to minimal media,

between PAO1 and PAO1 Δ*colR* in minimal media, and between PAO1 and PAO1 Δ*colR* in the rhizosphere. To determine if any individual *colR*-dependent genes are required for rhizosphere colonization, I screened mutants from a PAO1 two-allele transposon insertion library (76).

3. Identify rhizosphere stresses that may limit the growth of PAO1 Δ*colR*.

Due to the impaired tolerance of *P. putida colRS* mutants to environmental toxins (64, 69, 77), I hypothesized that ColRS may be required for tolerance against abiotic stresses in the rhizosphere. I characterized the growth of PAO1 Δ*colR* compared to wildtype PAO1 in media containing stressors that, based on functional gene analysis of the results from RNA-seq (described in previous objective) and literature, may be responsible for limiting the growth of PAO1 Δ*colR* in the rhizosphere environment. Because ColRS in *P. putida* is required for tolerance to transition metals, I hypothesized that metal tolerance was a conserved function of ColR in *P. aeruginosa* as well. Because the rhizosphere is generally acidic due to organic acids secreted by both the plant and bacteria, and LPS modifications and outer membrane proteins have been implicated in tolerance to low pH (78, 79), I hypothesized that PAO1 Δ*colR* would have a growth defect at low pH. I tested these hypotheses by characterizing the growth of PAO1 and PAO1 Δ*colR* in media with the addition of iron, zinc, manganese, and copper, and in media at acidic pH.

Chapter 2: ColR promotes *P. aeruginosa* rhizosphere colonization through regulation of novel colonization factors and increased abiotic stress tolerance.

2.1 Materials and Methods

2.1.1 Bacteria strains, media, and growth conditions

Bacteria strains and plasmids are listed in Table S1. All mutants listed in Table 2 were obtained from the PAO1 two-allele library (76). Routine bacterial culturing was performed using LB broth or agar at 37˚C. When appropriate, LB was supplemented with 10% sucrose, 15 µg/ml (*E. coli*), 50 µg/ml [*P. aeruginosa* PAO1 (14)], or 500 µg/ml [*P. aeruginosa* LESB58 (18)] gentamicin (Gm), 300 µg/ml carbenicillin (Cb), and 25 µg/ml Irgasan.

2.1.2 Strain construction

E. coli DH5α was used for construction and maintenance of plasmids, and *E. coli* SM10 λpir was used for biparental conjugation with *P. aeruginosa*. Deletion mutants were generated using the two-step allelic exchange method (80). Deletion constructs for PAO1 Δ*colR*, Δ*colS*, Δ*eptA*, and LESB58 Δ*colR* were generated using primers listed in Table S2. As the flanking regions have 100% sequence identity, the same deletion construct for Δ*colR* was used to make PAO1 Δ*colR* and LESB58 Δ*colR*. Approximately 700 bp of sequence flanking the target genes were amplified using PCR. The flanking regions were joined using overlap extension PCR (81). The PCR products were digested using the appropriate restriction enzymes and ligated into the multiple cloning site of pEXG2 suicide vector containing *sacB* (82). After confirming the insert by Sanger sequencing, the vector was transformed into *E. coli* SM10 λpir for conjugation into

PAO1 or LESB58 and integration into the genome through homologous recombination. *P. aeruginosa* merodiploids were selected using Gm and Irgasan. Counter-selection on plates with LB and sucrose was performed to select for loss of the plasmid, and colony PCR using the appropriate confirmation primers was used to screen for deletion mutants.

PAO1 and PAO1 Δ*colR* with empty vector (EV) were generated by electroporation with the broad host range expression plasmid with a Gm resistance marker, PBBR1MCS-5 (83). The *colR* complementation plasmid (pcolRnp) was created using the PBBR1MCS-5 plasmid as a backbone. PAO1 *colR* and approximately 200 bp upstream of the gene was amplified using primers listed in Table S2. Amplicon and plasmid were digested with the appropriate enzymes and ligated, and the resulting insert was confirmed by Sanger sequencing. The *colR* complementation strain was generated by electroporating pcolRnp into the PAO1 Δ*colR* mutant. Gm was used for selection and maintenance of the plasmid.

GFP-expressing *P. aeruginosa* were generated by electroporating strains with pSMC21 (*Ptac-GFP*) (84). Electrocompetent cells were prepared by pelleting, washing and resuspending cultures in 300 mM sucrose. Transformants were selected on and maintained using Cb.

2.1.3 Plant growth conditions

Axenic plants were generated by surface sterilizing Arabidopsis (wildtype accession Col-0) seeds in 70% ethanol for approximately 2 min, 10% bleach for approximately 2 min, and washed three times with sterile water (H_2O). Seeds were resuspended in H_2O and stored at 4˚C in the dark for at least 48h before plating on either solid Murashige and Skoog (MS) agar or liquid media (85), as described below. Plants were grown at 16h light/8h dark cycle and 22˚C.

2.1.4 Rhizosphere colonization in 48-well plates

Plants were grown hydroponically in flat-bottom 48-well plates as described (52, 86). Briefly, disks cut out of Teflon mesh were sterilized by autoclaving and placed in each well of a 48-well plate containing 250-300 µl MS plant growth media supplemented with 2% sucrose at pH 5.8. Sterilized Arabidopsis seeds were placed individually in the center of each disk. Plant media was changed to 270 µl of ½X MS media at pH 5.8 without sucrose after 10 days. At 12 days, overnight cultures of GFP-expressing bacteria were diluted to an OD_{600} of 0.0002 in 10 mM $MgSO_4$, and 30 µl was inoculated into each well to a final OD_{600} of 0.00002. GFP fluorescence (485 nm/535 nm excitation/emission) was read from the bottom of the wells each day up to 5 days post-inoculation, using a SpectraMax i3x fluorescent plate reader (Molecular Devices). Bacterial growth on a minimum of 15 plants was measured for each strain per experiment.

A standard curve of GFP fluorescence vs. OD_{600} was constructed and fitted to a linear equation to estimate bacterial abundance in the rhizosphere (Figure S1A). A separate linear equation was used for the complementation strains that harbour two plasmids (pSMC21 and PBBR1MCS-5) (Figure S1B), because of possible differences in plasmid copy number due to the presence an additional expression vector.

Screening of the Manoil lab PAO1 two-allele library transposon insertion mutants (76) for rhizosphere colonization defects were performed similarly, but OD_{600} of the liquid media from each well was measured instead of GFP fluorescence. Non-GFP-expressing bacteria were inoculated into wells containing 12-day-old plants to a final OD_{600} of 0.0002. At 5 days post-inoculation, 80 µl of media were transferred from each plant well into a 96-well plate. PAO1 and PAO1 Δ*colR* were included in each experiment as controls. OD_{600} readings were taken from the

96-well plate using SpectraMax i3x. A minimum of 8 wells were measured per strain. The ratio of mutant to wildtype colonization was estimated by dividing mutant OD_{600} over PAO1 OD_{600} after subtraction of the blank reading. Mutants with a OD_{600} ratio of below 0.7 relative to PAO1 were considered candidates for rhizosphere colonization defects and were retested using the GFP method above.

2.1.5 Study approval and animals

Animal experiments were performed by Morgan Alford and Daniel Pletzer in accordance with the Canadian Council on Animal Care (CCAC) guidelines following approval by the University of British Columbia Animal Care Committee (A14-0253). Mice used in this study were outbred CD-1 mice (female, 7-8 weeks). All animals were purchased from Charles River Laboratories, Inc. (Wilmington, MA). Mice weighed 25 ± 5 g at the experimental endpoint. Animals were group housed in cohorts of 4-5 littermates exposed to the same pathogen. Littermates were randomly assigned to experimental groups and standard animal husbandry protocols were employed.

2.1.6 Murine subcutaneous abscess infection model

The role of ColR in virulence during high density infection was examined using the less motile *P. aeruginosa* LESB58 (18) in a subcutaneous model of abscess infection (17). Briefly, the LESB58 wild-type (WT) or Δ*colR* mutant strain, as well as a *colR* complement or vector-only (PBBR1MCS-5) control strain, were sub-cultured at 37°C with shaking (250 rpm) to an OD_{600} = 1.0 in LB. Cells were washed twice with sterile phosphate buffered saline (PBS) and resuspended to a final OD_{600} = 1.0. Bacteria were injected (50 µl) subcutaneously into the left

dorsum of mice for an inoculum density of ~5.0 x 10^7 CFU. Abscesses were formed for 72 h with daily clinical grading. At the experimental endpoint, mice were euthanized by CO_2 and cervical dislocation. Visible dermonecrosis was measured using a caliper and abscesses were harvested in PBS. Then tissues were homogenized using a Mini-Beadbeater (BioSpec Products, Bartlesville, OK) for bacterial enumeration on LB following serial dilution. Two or three independent experiments containing 2-4 biological replicates each were performed (n = 5-10).

2.1.7 Bacterial RNA extraction, RNA-Seq, and qRT-PCR

RNA from rhizosphere-growing and minimal media-growing *P. aeruginosa* PAO1 was extracted for RNA-seq analysis. M9 minimal media supplemented with 24 mM L-glutamine (L-gln) was used as the minimal media control. Plants were grown hydroponically as described in the 48-well plate rhizosphere colonization assay. Wells containing 12-day-old plants were inoculated with PAO1 or PAO1 Δ*colR.* Because of difficulty extracting sufficient RNA for sequencing, a higher bacterial OD_{600} was used (final OD_{600} of 0.2 instead of 0.00002 for bacterial quantification above). PAO1 or PAO1 Δ*colR* were inoculated into 48-well plates containing M9 + 24 mM L-gln also to a final OD_{600} of 0.2. Both plant and minimal media plates were incubated in the plant growth conditions described above for 6 hours. After 6 hours, media from 6 plant wells or media from 3 minimal media were pooled and stabilized in RNAprotect® Bacteria Reagent (QIAGEN) before performing RNA extraction using RNeasy Mini Kit (QIAGEN). When necessary, RNA was concentrated using ethanol precipitation.

RNA from three biological replicates were used with RNA integrity numbers (RIN) ranging from 9.9 to 10.0. cDNA library preparation and RNA-sequencing using paired-end 150 bp reads were performed by GENEWIZ using Illumina HiSeq. The sequencing yielded an

average of 16,897,599 (standard deviation = 429,191) reads for each sample. The quality of the reads was assessed using FastQC v.0.11.8 (87). Salmon v.1.1.0 (88) was used to align reads the PAO1 transcriptome and to obtain the count files for each sample. Reads were mapped to the PAO1 transcriptome with an average mapping rate of 70.8% (standard deviation = 1.3%) for each sample. DESeq2 v1.26.0 was used for differential expression analysis in R (89). Log_2 fold change values were corrected using the *apeglm* package in R (90). Genes with log_2 fold change $\geq$ 0.585 and $\leq$ -0.585 ($\pm$ 1.5 fold change) and adjusted p-value (padj) $\leq$ 0.05 were considered significantly differentially expressed. The dittoSeq package was used to generate a heatmap of gene counts for genes that have higher expression in PAO1 than PAO1 Δ*colR* (91).

For qRT-PCR, RNA extractions were performed as described for RNA-seq. DNA depletion of the RNA samples was done using Turbo DNA-free kit (Invitrogen) and cDNA was generated using Superscript III Reverse Transcriptase (Invitrogen). PowerUp™ SYBR™ Green Master Mix (Applied Biosystems) was used for qRT-PCR reactions. Primers used in qRT-PCR are listed in Table S3. Relative gene expression was determined using ΔΔCt and normalizing to expression of the housekeeping gene *gyrB* (92).

2.1.8 Functional analysis of RNA-seq results

Kyoto Encyclopedia of Genes and Genomes (KEGG) pathway enrichment analysis was conducted using GAGE (93), using significantly differentially expressed genes in the rhizosphere compared to minimal media. Analyses for differentially expressed genes in PAO1 and PAO1 Δ*colR* in the rhizosphere compared to minimal media were conducted separately to obtain significantly enriched pathways for each strain. Pathways were filtered for significance based on a q-value $\leq$ 0.1.

PAO1 genes that were significantly differentially expressed in the rhizosphere vs. in M9 minimal media were divided into genes with higher and lower expression in the rhizosphere vs. M9 for GO term enrichment using the hypergeometric test in GOfuncR (94). Significantly enriched GO terms with FWER (family-wise error rate) ≤ 0.1 were refined to include only those with refined p-value ≤ 0.005.

2.1.9 Minimum inhibitory concentration (MIC) of transition metals

LB media supplemented with 2X the highest concentration of metals ($ZnSO_4$, $MnSO_4$, $FeSO_4$, and $CuSO_4$) to be used for the MIC assay were prepared. The solutions of LB + metal were serially diluted by 2X down the rows of round-bottom 96-well plates. The final volume in each well was 50 µl. Overnight bacterial cultures in LB were resuspended in fresh LB and diluted to an OD_{600} of 0.04. 50 µl of diluted bacterial cultures were added to each well. The 96-well plates were placed in an incubator at 37 ˚C for 24h before assessment of MIC. The MIC values were determined by eye and scored as the lowest concentration of metals in which there was at least a 50% reduction in growth.

2.1.10 Zinc tolerance plate assay

Zinc tolerance of the PAO1 Δ*colR* and LESB58 Δ*colR* mutants with empty vector or *colR* complementation vector were visually evaluated on LB agar plates containing 3 mM $ZnSO_4$. Overnight cultures of bacteria were pelleted and resuspended in fresh LB. The cultures were then serially diluted by tenfold and 10 µl of each dilution was spotted on LB plates with zinc. Cultures were also plated on LB plates without zinc as a control. Plates were incubated at 37˚C

for 24h (PAO1) or 48h (LESB58). Plates with LESB58 were incubated longer because of their slower growth rate.

2.1.11 *In vitro* growth assays

For all growth curves, bacterial cultures were pipetted into clear, flat-bottom 96-well plates to a final OD_{600} of 0.02 and a final volume of 100 µl. Growth was monitored using a shaking plate reader (Molecular Devices VersaMax microplate reader), at a fixed temperature of 37 ˚C. OD_{600} readings were taken once every 15 min for 24h. Each growth curve was repeated 3 times. Doubling times during the exponential growth stage were calculated using an online tool (http://www.endmemo.com/bio/bacteriagrowth.php) for each experiment and data reported are the average and standard deviation of 3 biological replicates. Significant differences in doubling times and lag phases were determined using t-tests assuming unequal variance.

Growth curves in ½X MS or M9 salts were performed similarly. L-gln at 24 mM was used as the carbon source in M9 minimal media. For growth curves at varying pH, ½X MS with 16 mM L-gln or 20 mM succinate was adjusted to pH 5, 6, or 7 using KOH. Overnight bacterial cultures in LB were washed and resuspended in 10 mM $MgSO_4$ and diluted to an OD_{600} of 0.2. 90 µl of sterile media were aliquoted into each well in a 96-well plate before inoculation with 10 µl of the diluted bacterial suspension.

Growth in $FeSO_4$, $ZnSO_4$, $MnSO_4$, and $CuSO_4$ were assessed by addition of the appropriate concentration of metals to LB. Metal concentrations used were below the MIC for both PAO1 and PAO1 Δ*colR*. LB containing twice the desired final concentration of the metal were added to each well to a final volume of 50 µl. Overnight bacterial cultures in LB were

pelleted, washed, and resuspended in fresh LB and diluted to an OD_{600} of 0.04. 50 µl of diluted bacterial cultures were added to the 50 µl of LB + metal in each well.

2.2 Results

2.2.1 *colRS* is required for *Pseudomonas aeruginosa* to colonize the Arabidopsis rhizosphere.

Thanks to its versatility, *P. aeruginosa* is naturally found in many environments, including soil and in association with plants (33, 34, 95). Various plants, including the model plant Arabidopsis, have been used as a host for studies of *P. aeruginosa* virulence (11, 30). Though the reference *P. aeruginosa* strain PAO1 is a clinical isolate, this strain has been reported to colonize plant rhizosphere as efficiently as the rhizosphere isolate *P. fluorescens* F113 and can cause disease symptoms in Arabidopsis (39).

To test whether ColRS, previously shown to be required for *P. fluorescens* rhizosphere colonization (50), is also required for rhizosphere colonization in *P. aeruginosa,* clean deletions of the regulator *colR* and the sensor kinase *colS* were generated in the *P. aeruginosa* reference strain PAO1 (subline H103) (14). Rhizosphere colonization was quantified using a previously described 48-well GFP fluorescence-based rhizosphere colonization assay (86). Plants hydroponically growing in 48-well plates were inoculated with PAO1 mutant strains expressing GFP. The fluorescence signal at day 5 post-inoculation was measured and converted to OD_{600} using a calibration curve (Figure S1) to estimate bacterial growth in the rhizosphere.

I found that both the PAO1 Δ*colR* and Δ*colS* mutants have significantly lower growth in the Arabidopsis rhizosphere compared to wildtype PAO1 (Figure 2A and B). On average, PAO1

Δ*colR* grew to approximately 6% of wildtype levels, while PAO1 Δ*colS* grew to approximately 4% of wildtype levels. PAO1 Δ*colR* did not have a growth defect in minimal media, suggesting that it does not have a general growth defect (Figure S2). Because *colS* and *colR* are two components of the same signaling pathway, and deletion of *colS* and *colR* in PAO1 led to similar rhizosphere colonization defects, only PAO1 Δ*colR* was used for the remainder of this study.

To confirm this rhizosphere colonization defect of the PAO1 Δ*colR* mutant was directly due to loss of *colR*, I complemented PAO1 Δ*colR* with a wildtype copy of *colR* expressed by its native promoter. Because reduced zinc tolerance is a known phenotype of *P. aeruginosa* lacking *colR* (70), I used this phenotype to quickly confirm the ability of a plasmid containing the *colR* open reading frame and approximately 200 bp upstream (pcolRnp) to complement the zinc tolerance defect of PAO1 Δ*colR* (Figure S3A). I tested the same complementation strain for rhizosphere colonization and found that growth in the rhizosphere was restored in PAO1 Δ*colR* with pcolRnp, and not with the empty vector (EV) (Figure 2C).

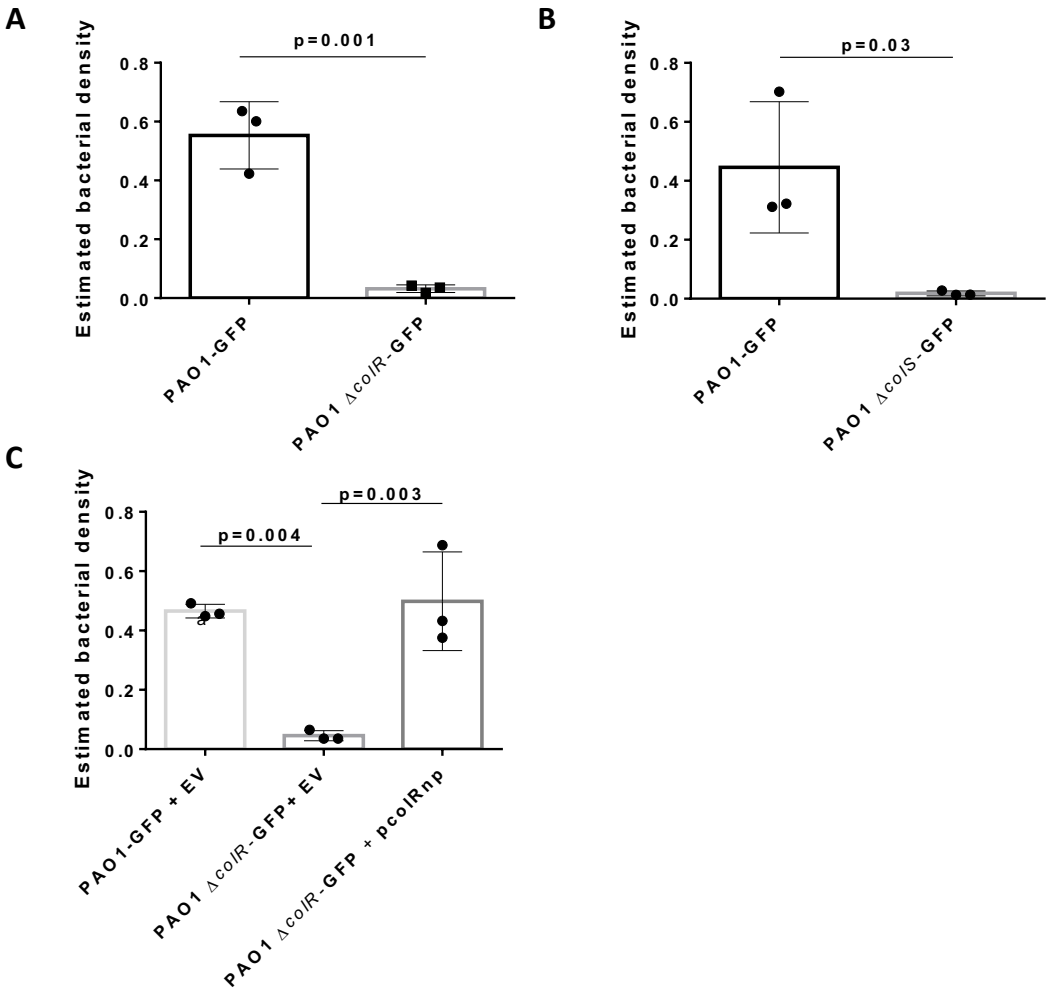

Figure 2. The *colRS* two-component system in *P. aeruginosa* is required for colonization of Arabidopsis rhizosphere. (A-B) To measure bacterial rhizosphere colonization levels, 12-day-old plants growing hydroponically in 48-well plates were inoculated with GFP-expressing *P. aeruginosa* PAO1 and **(A)** PAO1 Δ*colR* or **(B)** PAO1 Δ*colS*. **(C)** Rhizosphere colonization of GFP-expressing PAO1 or PAO1 Δ*colR* containing empty vector (EV) or the *colR* complementation vector (pcolRnp). GFP fluorescence values in each plant-containing well were measured 5 days post-inoculation, and fluorescence values were converted to OD_{600} using a calibration curve. Data points in each graph represent the mean OD_{600} values of independent experiments and error bars represent standard deviation. P-values were calculated using pairwise t-tests (A and B) or analysis of variance (ANOVA) and Turkey's honest significant difference (HSD) test (C).

2.2.2 *P. aeruginosa colR* is required for virulence in a mouse subcutaneous abscess model.

Because similar bacterial traits were found to be important for colonization of both plants and animals, we wondered whether *colR* is also required for colonization and persistence during chronic infection in a mouse model, for which findings have potentially clinically relevant implications. As mentioned in Chapter 1, a subcutaneous mouse abscess model was developed by Pletzer *et al.* for studying and monitoring localized chronic infections by clinically important Gram-negative bacteria, including *P. aeruginosa* (17).

The chronic infection isolate LESB58 was the *P. aeruginosa* strain used in this model instead of PAO1. Even though LESB58 is hypervirulent in humans, it exhibits poor swimming motility and has slower growth rate *in vitro* than PAO1 or PA14, allowing LESB58 to establish a localized abscess infection rather than disseminating and causing high mice mortality (17). Either wildtype LESB58 or the Δ*colR* mutant (LESB58 Δ*colR*) were subcutaneously injected into backs of mice, forming an abscess upon establishment of infection (17). Interestingly, we found that the LESB58 and LESB58 Δ*colR* colonized the abscess to similar extent 3 days post-infection as measured by CFUs recovered from the abscess, but LESB58 Δ*colR* formed significantly smaller abscesses (Figure 3A). This suggests that *colR* may regulate genes required for virulence rather than growth in the abscess.

Introduction of wildtype *colR* into the LESB58 Δ*colR* mutant using pcolRnp did not restore the abscess size to the levels caused by infection with wildtype LESB58 (Figure 3B). In contrast, infection with the complementation strain (LESB58 Δ*colR* + $pcolR_{np}$) produced a smaller abscess size than infection with the Δ*colR* mutant with an empty vector (LESB58 Δ*colR* + EV). To ensure this result was not due to an inability of the plasmid to complement in

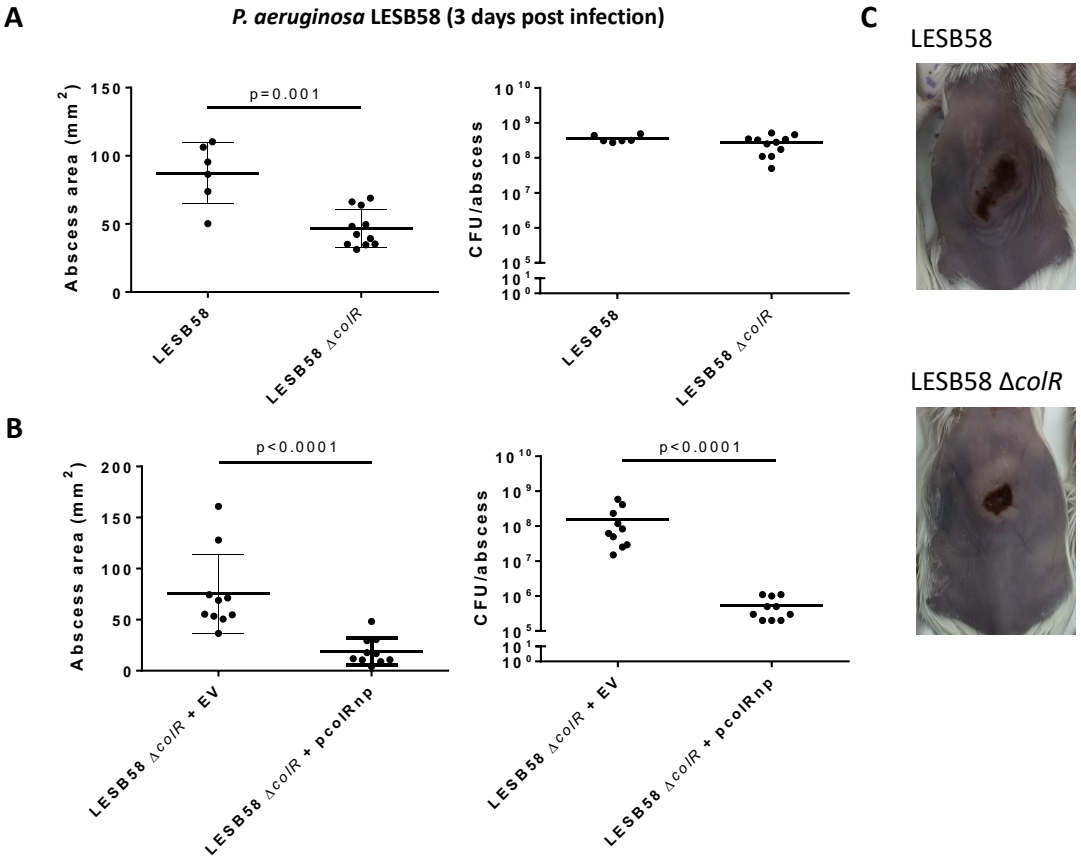

Figure 3. ColR is required for virulence and affects colonization of LESB58 in a murine subcutaneous abscess infection. (A) Wildtype LESB58 and the Δ*colR* mutant or **(B)** LESB58 Δ*colR* harbouring empty vector (EV) or pcolRnp were injected (~5 x 10^7 CFU inoculum) into the subcutaneous thin skeletal muscle on the dorsum of mice. Abscess lesion size and CFU counts were determined 3 days post infection. Error bars represent standard deviation. P-values were determined using Mann-Whitney U tests. **(C)** Representative images of abscesses formed by wildtype LESB58 and the Δ*colR* mutant. Images were taken 3 days post infection. Data presented in this figure were obtained by Daniel Pletzer and Morgan Alford.

LESB58, I confirmed that pcolRnp was also able to restore the zinc tolerance phenotype of LESB58 Δ*colR* (Figure S3B). In addition, growth of LESB58 Δ*colR* + $pcolR_{np}$ in the abscess was significantly impaired relative to LESB58 Δ*colR* + EV. The complementation of *colR* on plasmid likely increased the copy number of *colR* mRNA and amount of ColR in the cell. Excess ColR in the cell could explain the failure to complement the virulence phenotype, through over-expression or over-repression of genes in the ColR regulon, or other unforeseen effects on ColR-dependent gene expression.

Given that loss of *colR* resulted in decreased virulence of LESB58 in the murine abscess, this demonstrated that the *in vivo* importance of *colR* in *P. aeruginosa* was not limited to the Arabidopsis rhizosphere. Identifying *colR*-dependent mechanisms necessary for *P. aeruginosa* plant colonization could potentially identify novel virulence determinants in animal infections.

2.2.3 The ColRS-regulated gene, *eptA*, encoding a phosphoethanolamine transferase, is not required for growth in the rhizosphere.

A gene previously found to be regulated by *P. aeruginosa* ColRS is *eptA*, which is induced in response to zinc stress (70). EptA is one of three predicted phosphoethanolamine (pEtN) transferases in *P. aeruginosa* but is the only one that can modify lipid A (70). PEtN addition to lipid A provides resistance to the cationic antibiotic polymyxin B in some bacteria, including in *Salmonella* and in *Vibrio* spp. (96, 97), though induction of *eptA* does not affect polymyxin B resistance in *P. aeruginosa* (70). It is unknown what benefit *eptA* provides for *P. aeruginosa*, as *eptA* is not required for zinc tolerance (70). I hypothesized that pEtN addition to the outer membrane could be necessary for *P. aeruginosa* survival in the rhizosphere, for example, for protection against entry of cationic defense peptides present in root exudates (98).

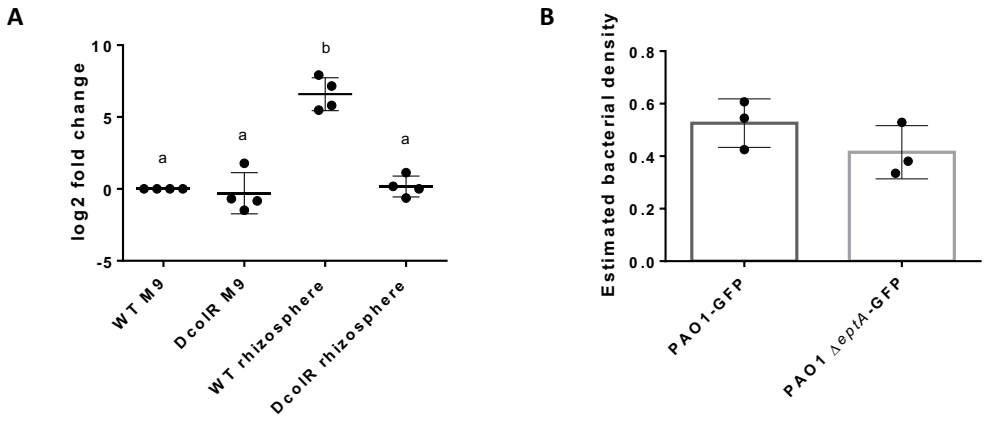

Figure 4. *EptA* is induced in the rhizosphere in a *colR*-dependent manner but is not required for rhizosphere colonization. (A) qRT-PCR of *eptA* expression levels in the PAO1 and the Δ*colR* mutant relative to *eptA* expression in PAO1 in M9 minimal media, using RNA extracted from samples in 4 biological replicates. Log_2 fold changes were determined by calculating ΔΔCt. The housekeeping gene *gyrB* was used to normalize cDNA quantities between samples. Letters designate levels of significance by ANOVA and Turkey's HSD test ($p < 0.05$). **(B)** Rhizosphere colonization of the GFP-expressing PAO1 and the Δ*eptA* mutant. GFP fluorescence values measured in each well at 5 days post-inoculation were converted to OD_{600} using a calibration curve. Data points in each graph represents mean measurements of independent experiments. Error bars represent standard deviation.

Using quantitative reverse transcriptase PCR (qRT-PCR), I found that there is *colR*-dependent induction of *eptA* expression in rhizosphere-growing *P. aeruginosa* PAO1 (Figure 4A). At 6 hours post-inoculation, PAO1 *eptA* is induced by an average log_2 fold change of approximately 6.6 in the rhizosphere compared to M9 minimal media. In addition, the induction of *eptA* in the rhizosphere is completely absent in a PAO1 Δ*colR* mutant at 6 hours in the rhizosphere. This indicates that *eptA* is induced in the rhizosphere in a *colR*-dependent manner.

To test whether *eptA* is necessary for rhizosphere colonization, I generated a clean deletion of *eptA* in PAO1 (PAO1 Δ*eptA*). I found that PAO1 Δ*eptA* does not have a significant reduction in rhizosphere colonization (Figure 4B), suggesting there must be distinct *colR*-dependent genes that are necessary for successful rhizosphere colonization.

2.2.4 Use of RNA-seq to identify *colR*-dependent transcriptional changes in the rhizosphere.

To identify additional *colR*-dependent genes in the rhizosphere that may contribute to successful rhizosphere colonization, I examined global transcriptomic profiles in PAO1 and PAO1 Δ*colR*. Differences in gene expression between PAO1 and PAO1 Δ*colR* in the rhizosphere could reveal genes that regulate host association. Comparing gene expression profiles of PAO1 in the rhizosphere to minimal media may also elucidate genes and processes that are important for adaptation to the rhizosphere including, metabolism of rhizosphere nutrients, and protection from deleterious compounds in the rhizosphere.

I used RNA-seq to examine the transcriptomes of wildtype PAO1 and the PAO1 Δ*colR* mutant. Transcriptional profiles of wildtype PAO1 and the Δ*colR* mutant were compared in both the rhizosphere and in M9 minimal media, in which PAO1 Δ*colR* does not show a growth defect compared to PAO1 (Figure S2). Bacterial RNA from 6 hours post-inoculation was collected to capture differences in early transcriptional responses to the root environment between wildtype PAO1 and PAO1 Δ*colR*. Six hours post-inoculation is a timepoint before there was a dramatic enough difference in growth of the Δ*colR* mutant vs. wildtype in the rhizosphere to impact RNA yields, but sufficient time for *colR*-dependent gene expression to be observed in the rhizosphere (Figure 4A). RNA was extracted and sequenced on an Illumina HiSeq. Three biological replicates were sequenced per bacterial genotype and condition and approximately 17 million reads were obtained, with an average mapping rate of 70.8% to the PAO1 genome (see Methods for details).

2.2.5 Loss of *P. aeruginosa* PAO1 *colR* has little impact on global transcriptional changes in minimal media or in the rhizosphere.

To visualize the variation in gene expression across samples, I generated a principal component analysis (PCA) plot using the count matrix of the transcripts in each sample. Approximately 94% of the variance between samples is explained by the different growth conditions (M9 vs. rhizosphere), while difference in bacteria genotype (wildtype *P. aeruginosa* PAO1 vs. the Δ*colR* mutant) accounts for less than 2% of sample variance (Figure 5A). The high variance between gene expression of M9 and rhizosphere bacteria samples are visualized by their distinct clustering in the PCA plot, showing that minimal media and the rhizosphere are distinct environments for bacterial growth. Additionally, PAO1 and PAO1 Δ*colR* samples cluster separately in the PCA plot only in the rhizosphere and not in the M9 minimal media control (Figure 5A). This result indicates that dysregulation of genes from the loss of *colR* at 6 hours is more pronounced in the rhizosphere than in minimal media.

To identify genes induced in the rhizosphere, and genes with *colR*-dependent expression, I identified differentially expressed genes in the following comparisons: 1) PAO1 in M9 vs. PAO1 in the rhizosphere, 2) PAO1 Δ*colR* in M9 vs. PAO1 Δ*colR* in the rhizosphere, 3) PAO1 vs. PAO1 Δ*colR* in M9, and 4) PAO1 vs. PAO1 Δ*colR* in the rhizosphere (Figure 5B).

In the first two comparisons, I found that relative to growth in M9, growth in the rhizosphere induced large-scale changes in the transcriptomes of both wildtype PAO1 and the PAO1 Δ*colR* mutant, with up- and down-regulation of approximately 50% of the total transcripts encoded in the PAO1 genome. Consistent with the most pronounced changes in gene expression being between the rhizosphere and M9 minimal media, similar numbers of genes were up- and down-regulated in PAO1 and PAO1 Δ*colR* in the rhizosphere vs. M9 (Figure 5B). This included

1445 and 1467 genes up-regulated in PAO1 and PAO1 Δ*colR* respectively, and 1524 and 1478 genes down-regulated in PAO1 and PAO1 Δ*colR* respectively (Figure 5B). In addition, most of the genes with higher or lower expression in the rhizosphere relative to M9 were shared between both wildtype PAO1 and the PAO1 Δ*colR* mutant. Of the total number of genes up-regulated in the rhizosphere, 71.8% were shared between PAO1 and PAO1 Δ*colR* (1217 out of 1695). Of the total number of genes down-regulated in the rhizosphere, 81.9% were shared between PAO1 and PAO1 Δ*colR* (1352 out of 1650) (Figure 5B). These results, along with the PCA, suggest that even though there is a significant difference in the abilities of PAO1 and PAO1 Δ*colR* to grow in the rhizosphere, ColR is likely not a global regulator of genes involved in rhizosphere colonization.

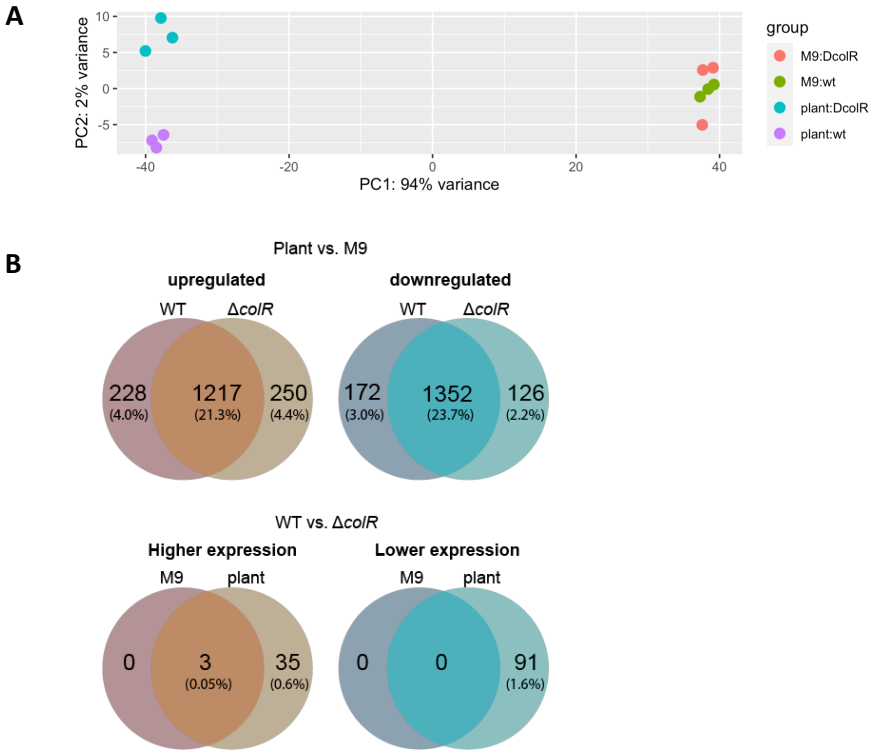

Figure 5. Gene expression profiles of *P. aeruginosa* PAO1 growing in the rhizosphere are distinct from those of PAO1 in M9 minimal media. (A) PCA plot of transcript count matrices to visualize the variation in gene expression profiles of wildtype PAO1 and the PAO1 Δ*colR* mutant in minimal media and the rhizosphere. Counts used to make the PCA plot were first transformed using variance stabilizing transformation. **(B)** Venn diagram of the number and percentage of total transcripts encoded in the PAO1 genome of significantly differentially expressed genes (greater than 1.5-fold change, padj < 0.05). (Top) Differentially expressed genes between the rhizosphere and M9 minimal media that are shared between or unique to wildtype PAO1 and the Δ*colR* mutant. (Bottom) Differentially expressed genes between PAO1 and the Δ*colR* mutant that are shared between or unique to the rhizosphere (plant) and M9 conditions.

Analysis of the predicted functions of genes induced or repressed in the rhizosphere relative to M9 may identify bacterial pathways required for metabolism and protection against plant defense compounds. Pathway enrichment analysis was performed on KEGG pathways assigned to the genes up- and down-regulated in the rhizosphere relative to minimal media (Figure 6). The transcriptomes of both PAO1 and PAO1 Δ*colR* were significantly enriched in the

same KEGG pathways in the rhizosphere relative to M9 (q-value < 0.1). Genes with significant up-regulation in the rhizosphere were enriched for predicted functions related to carbon metabolism including starch and sucrose metabolism and the pentose phosphate pathway. Significantly down-regulated genes in the rhizosphere relative to M9 were enriched for predicted functions in biofilm formation, bacterial secretion systems, sulfur metabolism, ABC transporters, and the formation of ribosomes. Phenazine biosynthesis was the only pathway that was identified in the PAO1 but not the PAO1 Δ*colR* transcriptome (q-value = 0.18). This analysis shows major differences in carbon and nutrient metabolism between bacteria growing in the rhizosphere vs. M9. While M9 L-gln minimal medium has L-gln as the sole carbon source, there is a greater diversity of organic compounds in root exudate (46, 99). Increase in starch and sucrose metabolism may indicate that these carbon sources are being similarly metabolized by both PAO1 and the PAO1 Δ*colR* mutant.

Though there were 228 genes that were up-regulated in PAO1 in the rhizosphere that were not up-regulated in PAO1 Δ*colR*, and 172 genes that were down-regulated in the PAO1 in the rhizosphere that were not down-regulated in the Δ*colR* mutant (Figure 5B), many of these genes trend towards being up- or down-regulated in both PAO1 and PAO1 Δ*colR* but did not make the 1.5-fold change cut-off in the PAO1 Δ*colR* mutant. As I aimed to find *colR*-dependent

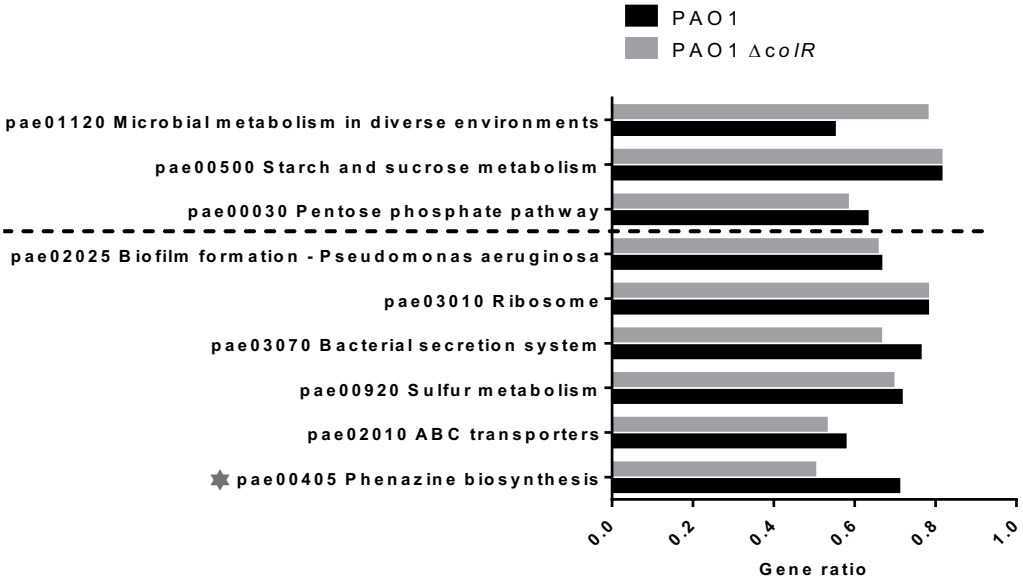

Figure 6. Enriched KEGG pathways in the rhizosphere vs. minimal media are similar in wildtype *P. aeruginosa* PAO1 and the Δ*colR* mutant. Significantly enriched KEGG pathways (q-value ≤ 0.1) were identified using GAGE analysis of the significantly differentially expressed genes (± 1.5-fold change, padj < 0.05) in PAO1 and PAO1 Δ*colR* in the rhizosphere compared to M9 minimal media. The gene ratio is the ratio of genes assigned to a given KEGG pathway to the total number of genes annotated to the pathway in the PAO1 genome. Pathways above the dotted line are up-regulated in the rhizosphere vs. M9, and the pathways below the dotted line are down-regulated. The star indicates phenazine biosynthesis, the only pathway that was significantly enriched in PAO1 but not in PAO1 Δ*colR*.

genes that contribute to the growth defect of PAO1 Δ*colR* in the rhizosphere, I decided to focus on the differentially expressed genes identified by directly comparing gene expression between wildtype PAO1 and the PAO1 Δ*colR* mutant in the rhizosphere.

2.2.6 *colR*-dependent gene expression in the rhizosphere

To identify genes induced in the rhizosphere in a *colR*-dependent manner, I compared the gene expression profiles between wildtype *P. aeruginosa* PAO1 and the PAO1 Δ*colR* mutant in M9 and in the rhizosphere. I identified 38 genes with significantly higher expression in PAO1 than in PAO1 Δ*colR* and 91 genes with significantly lower expression in PAO1 than in PAO1 Δ*colR* (± 1.5-fold change, padj < 0.05) (Figure 5B). Interestingly, only three genes: *colR* (PA4381), *colS* (PA4380) and PA4517, were significantly differentially expressed in between PAO1 and PAO1 Δ*colR* in M9 (Figure 5B). The absence of *colR* transcript in the Δ*colR* mutant under both conditions serves as a control for the analysis. Because *colS* is directly downstream of *colR* and transcribed in the same operon, transcript counts of *colS* could be negatively impacted by polar effects and decreased stability of the truncated mRNA. These results suggest that *colR* has a more pronounced regulatory role in PAO1 in the rhizosphere than in M9.

Genes that have higher expression in PAO1 compared to PAO1 Δ*colR* are of particular interest. These are genes that are likely positively regulated by ColR, and expression of these genes may be required for rhizosphere colonization. Only 38 genes had lower expression in the Δ*colR* mutant than in wildtype PAO1, the names and expression patterns of which are shown in a heatmap of relative gene counts in Figure 7. Many of these genes have products that localize to the periplasm or the cytoplasmic membrane. These include *tpbA* (PA3885), encoding a protein tyrosine phosphatase, *mntP* (PA2910), encoding a manganese efflux pump, and *nhaP* (PA3887), encoding a sodium-proton antiporter. The pEtN transferase-encoding gene *eptA* (PA1972) also had lower expression in the Δ*colR* mutant than in PAO1, which was an expected outcome of the analysis (70). Interestingly, the expression of another two genes encoding predicted pEtN transferases, PA4517 and PA3310, was also positively regulated by *colR* in the rhizosphere

(Figure 7). The targets of PA4517 and PA3310 have not yet been identified in PAO1, as they do not appear to modify lipid A like EptA (70). Other notable genes include *lip3* (PA2364) and *hsiC3* (PA2366), which encode proteins that function in the third type VI secretion system of PAO1 (H3-T6SS).

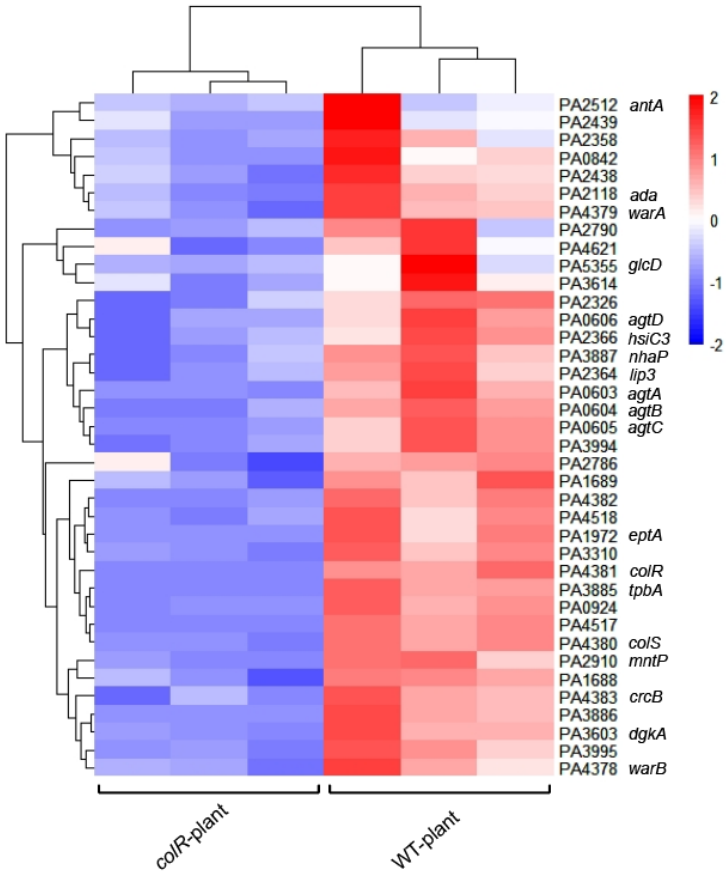

Figure 7. Heatmap showing genes with lower expression in the *P. aeruginosa* PAO1 Δ*colR* mutant in the rhizosphere compared to wildtype PAO1. Counts of genes with significantly lower expression in the Δ*colR* mutant compared to PAO1 in the rhizosphere (>1.5-fold change, padj < 0.05) are shown on a heatmap using dittoSeq (91). Gene counts that are higher than row average are shown in red, and gene counts that are lower than row average are shown in blue.

Genes that have lower expression in PAO1 compared to PAO1 Δ*colR* may be genes that are negatively regulated by ColR, or genes that are indirectly up-regulated to compensate for the loss of *colR*. The induction of alternative stress response pathways by loss of ColR was proposed

in *P. putida*, where the *colR* mutant proteome was affected much more by exposure to zinc than wildtype, likely to compensate for the loss of *colR*-dependent zinc tolerance pathways (100). I performed gene ontology (GO) enrichment analysis to identify functions significantly enriched in the products of genes negatively regulated by ColR. "Alginic acid biosynthesis" (GO:0042121) was one of the significantly enriched GO terms, and interestingly, an increase in alginate biosynthesis proteins was also observed in the *P. putida colR* mutant, but not in wildtype *P. putida* in response to zinc. This suggests that alginate biosynthesis may be a conserved mechanism to compensate for the lack of *colR* (100). The other significantly enriched GO terms are "response to stimulus" (GO:0050896, biological process), "transmembrane transporter activity" (GO:0022857, molecular function), "external encapsulating structure" (GO:0030312, cellular component), and "cell envelope" (GO:0030313, cellular component). Genes in the PAO1 genome assigned with the GO terms "alginic biosynthetic process", "response to stimulus", and/or "transmembrane transporter activity" that are significantly higher expressed in the Δ*colR* mutant vs. wildtype PAO1 are listed in Table 1. The GO terms, "external encapsulating structure" and "cell envelope", were excluded because of redundancy; many of the genes annotated to these GO terms were also assigned to "transmembrane transporter activity" or "response to stimulus". The functional categorization of negatively *colR*-dependent genes further supports the role of ColR in regulation of membrane functionality.

Table 1. GO categorization of genes that are negatively dependent on *colR* in the rhizosphere. Genes shown are 32 out of the 91 whose expression is negatively dependent on *colR*. Log_2 fold change of gene counts in PAO1 Δ*colR* compared to PAO1 in the rhizosphere are shown. Genes that belong to more than one GO category are listed more than once.

PAO1 locus	Gene name (if available)	Annotation/Predicted function	Log2 fold change
GO:0042121		**alginic acid biosynthetic process (biological process)**	

PA3540	*algD*	GDP-mannose 6-dehydrogenase	3.33
PA3542	*alg44*	Alginate biosynthesis protein	1.60
PA3543	*algK*	Alginate biosynthetic protein precursor	1.75
PA3544	*algE*	Alginate production outer membrane protein precursor	1.48
PA3547	*algL*	Poly(beta-d-mannuronate) lyase precursor	1.71
PA3549	*algJ*	Alginate o-acetyltransferase	1.16
PA3550	*algF*	Alginate o-acetyltransferase	1.60
PA3551	*algA*	Phosphomannose isomerase / guanosine 5'-diphospho-D-mannose pyrophosphorylase	1.44
PA5483	*algB*	Two-component response regulator	0.64
GO:0050896		**response to stimulus (biological process)**	
PA0320	*carO*	Calcium-regulated OB-fold protein	1.08
PA0425	*mexA*	RND multidrug efflux membrane fusion protein precursor	0.60
PA1959	*bacA*	Bacitracin resistance protein	0.87
PA2479		Two-component response regulator	0.75
PA2575		Nitroreductase (Interpro ID IPR00415)	1.72
PA2899	*atvR*	Atypical virulence-related response regulator	0.60
PA3540	*algD*	GDP-mannose 6-dehydrogenase	3.33
PA3542	*alg44*	Alginate biosynthesis protein	1.60
PA3543	*algK*	Alginate biosynthetic protein precursor	1.75
PA3544	*algE*	Alginate production outer membrane protein precursor	1.48
PA3547	*algL*	Poly(beta-d-mannuronate) lyase precursor	1.71
PA3549	*algJ*	Alginate o-acetyltransferase	1.16
PA3550	*algF*	Alginate o-acetyltransferase	1.60
PA3551	*algA*	Phosphomannose isomerase / guanosine 5'-diphospho-D-mannose pyrophosphorylase	1.44
PA3677	*mexJ*	RND efflux membrane fusion protein	0.76
PA3901	*fecA*	Fe(III) dicitrate transport protein	0.59
PA5159		Multidrug resistance protein	0.90
PA5160		Drug efflux transporter	0.83
PA5483	*algB*	Two-component response regulator	0.64
GO:0022857		**transmembrane transporter activity (molecular function)**	
PA0103		Sulfatase transporter	0.92
PA0425	*mexA*	RND multidrug efflux membrane fusion protein precursor	0.60
PA1212		Probable major facilitator superfamily (MFS) transporter	0.69
PA1777	*oprF*	Major porin and structural outer membrane porin OprF precursor	1.32
PA2041		Amino acid permease	0.77
PA2526	*muxC*	Efflux transporter	0.69
PA2527	*muxB*	RND efflux transporter	0.67
PA2528	*muxA*	RND efflux membrane fusion protein	0.75
PA3136		Secretion protein	0.87
PA3521	*opmE*	Outer membrane efflux protein	1.09
PA3523	*mexP*	RND efflux membrane fusion protein	1.12

PA3677	*mexJ*	RND efflux membrane fusion protein	0.76
PA3901	*fecA*	Fe(III) dicitrate transport protein	0.59
PA3920	*copA1*	Cu(II)-ATPase	0.78
PA4222		ATP-binding component of ABC transporter	0.60
PA5158	*opmG*	Outer membrane protein	0.97
PA5159		Multidrug resistance protein	0.90
PA5160		Drug efflux transporter	0.83

To confirm the RNA-seq results, I used qRT-PCR on a set of RNA samples independently obtained from those that were submitted for RNA-seq. By qRT-PCR, I found that genes with lower expression in the Δ*colR* mutant than in PAO1 including *eptA, tpbA*, PA3310, and *mntP* showed significant *colR*-dependent induction in the rhizosphere (Figure 4A, Figure 8A). In contrast, genes that had significantly higher expression in the Δ*colR* mutant than in PAO1 in the rhizosphere including *algD, algA*, and *azoR3*, did not show increased expression in the Δ*colR* mutant by qRT-PCR (Figure 8B). Though on average, expression of *algD* and *algA* were $\log_2$ fold changes of 0.9 and 1.3 higher in PAO1 Δ*colR* than in PAO1, the differences were not significant. *AzoR3*, was also found to have no difference in expression in the new samples using qRT-PCR. This suggests that expression of putatively negatively regulated *colR*-dependent genes may be compensating for the lack of ColR, and stochastic, rather than direct targets of ColR.

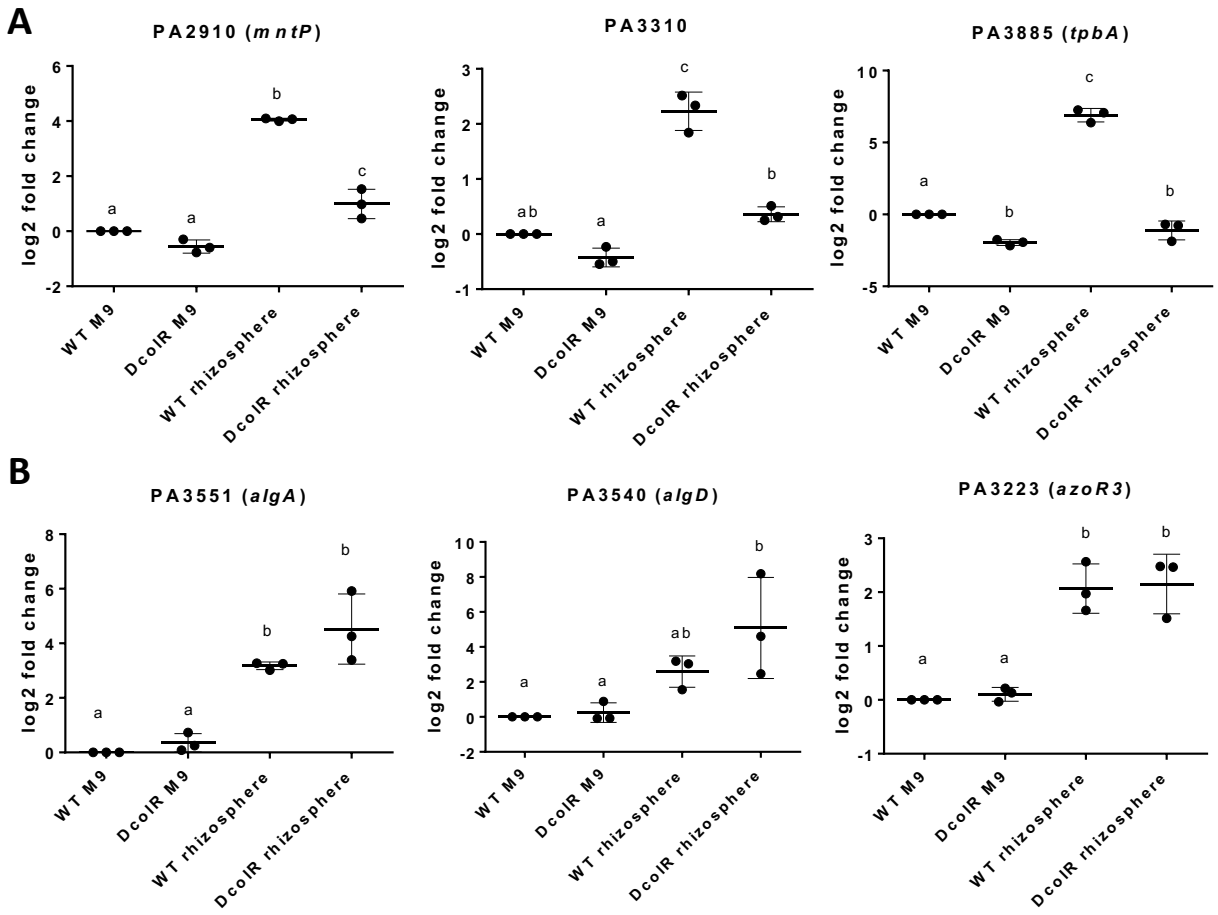

Figure 8. Expression of putatively ColR-dependent genes identified by RNA-seq. qRT-PCR was performed on a subset of genes identified by RNA-seq. Log_2 fold changes were determined by calculating ΔΔCt normalized to the housekeeping gene *gyrB*. Letters designate levels of significance determined by ANOVA and Turkey's HSD test ($p < 0.05$). **(A)** Select genes with higher transcript counts in PAO1 compared to the Δ*colR* mutant and **(B)** select genes with lower transcript counts in PAO1 compared to the Δ*colR* mutant, according to the RNA-seq analysis. qRT-PCR was performed on RNA from 3 biological replicates with 2 technical replicates each.

2.2.7 Identification of novel *colR*-dependent rhizosphere colonization factors.

Among the genes in the rhizosphere with *colR*-dependent expression, few genes have been studied in the context of host-colonization and thus presents opportunities to identify novel colonization factors. To identify ColR-dependent genes important for rhizosphere colonization, I developed an assay to rapidly assess whether disruption of any single *colR*-dependent gene in

PAO1 is sufficient to result in a rhizosphere colonization defect. Transposon insertion mutants from the Manoil lab PAO1 two-allele library (76) were screened for rhizosphere colonization defects by measuring the OD_{600} in the plant media 5 days after inoculation with bacteria (see Methods for details). Mutants screened and tested for rhizosphere colonization defects are listed in Table 2. For genes that are predicted to be in operons (PA0603-PA0606, PA4378-PA4379, PA2438-PA2439), transposon insertion mutants in the first transcribed gene were tested (PA0603, PA4379, PA2439). For genes in which there are multiple transposon insertion mutants available, the mutant with the earliest transposon insertion in its open reading frame was tested. Mutants with an average colonization of less than 70% of PAO1 as measured in this primary screen were candidates for having a colonization defect.

Table 2. Rhizosphere colonization of mutants in ColR-regulated genes. Mutants in genes with lower expression in wildtype PAO1 than in PAO1 Δ*colR* (log_2 fold change ≤ -0.585, padj ≤ 0.05) were screened for rhizosphere colonization defects.

Locus tag	Gene name (if available)	Description of gene product	Log2 Fold Change	Mutant	Candidate for rhizosphere colonization defect (<70% of the wildtype growth in primary screen)
PA3885	*tpbA*	Protein tyrosine phosphatase	-6.86	PW7555	**Yes**
PA4517		Phosphoethanolamine transferase	-5.24	PW8605	No
PA0924		Sulfuric ester hydrolase activity	-3.19	PW2676	**Yes**
PA3603	*dgkA*	Diacylglycerol kinase	-2.90	PW7119	**Yes**
PA2910	*mntP*	Manganese efflux pump	-2.78	PW3828	No
PA4518			-2.11	PW8607	**Yes**
PA3310		Phosphoethanolamine transferase	-1.53	PW6565	No
PA4382		Phosphatidic acid phosphatase (Interpro annotation)	-1.47	PW8402	**Yes**
PA0603	*agtA*	ABC transporter, polyamine transport	-1.42	PW2102	**Yes**
PA5355	*glcD*	Glycolate oxidase subunit	-1.41	PW10024	No
PA1688		Strictosidine synthase activity	-1.38	PW3999	No
PA3995		DNA-binding transcription factor	-1.07	PW7756	No
PA4379	*warA*	c-di-GMP-binding methyltransferase	-1.02	PW8396	No
PA2512	*antA*	anthranilate dioxygenase large subunit	-1.01	PW5208	No
PA3887	*nhaP*	Na+/H+ antiporter	-0.99	PW7558	No
PA2358			-0.85	PW4969	No
PA2366	*hsiC3*	Type VI secretion system tail sheath (Interpro annotation)	-0.78	PW4984	No
PA3614			-0.78	PW7139	No
PA0842		Probable glycosyl transferase	-0.67	PW2533	No
PA2439		Integral membrane component (GO annotation)	-0.67	PW5104	**Yes**
PA2790			-0.65	PW5671	**Yes**
PA3994		Probable epoxide hydrolase	-0.64	PW7754	No
PA4621		Probable oxidoreductase	-0.64	PW8784	**Yes**
PA4383	*crcB*	Integral membrane component, putative fluoride ion transporter (Interpro annotation)	-0.61	PW8404	No
PA2326		Monooxygenase activity (GO annotation)	-0.59	PW4923	**Yes**

Several transposon insertion mutants were identified as candidates for having a rhizosphere colonization defect, as indicated by the initial screen (Table 2). Five mutant candidates, PW7555 (*tpbA*::Tn5), PW2676 (PA0924::Tn5), PW7119 (*dgkA*::Tn5), PW8607 (PA4518::Tn5), and PW8402 (PA4382::Tn5), which had insertions in genes with the greatest difference in fold change in PAO1 Δ*colR* compared to PAO1 in the rhizosphere, were retested

using the rhizosphere colonization GFP assay. I found that mutants PW7555, PW7119, and PW8402, but not PW2676 and PW8407 had significantly decreased rhizosphere colonization compared to PAO1 (Figure 9). This suggests that *tpbA*, encoding a protein tyrosine phosphatase, *dgkA*, encoding a diacylglycerol kinase, and PA4382 encoding a type 2 phosphatidic acid phosphatase (PAP2) were required for rhizosphere colonization in our assay conditions. Both *dgkA* and PA4382 are likely involved in phospholipid biosynthesis and homeostasis (75), and homologs of both genes were also ColR-regulated in *P. putida* (63). *TbpA* is a novel *colR*-regulated gene identified in this study. *P. aeruginosa* TpbA is a negative regulator of cellular c-di-GMP and biofilm formation (101–103). These data indicate that *colR* is required for expression of multiple rhizosphere colonization factors including *tpbA*, *dgkA*, and PA4382, which explains the drastically reduced growth of the Δ*colR* mutant in the rhizosphere.

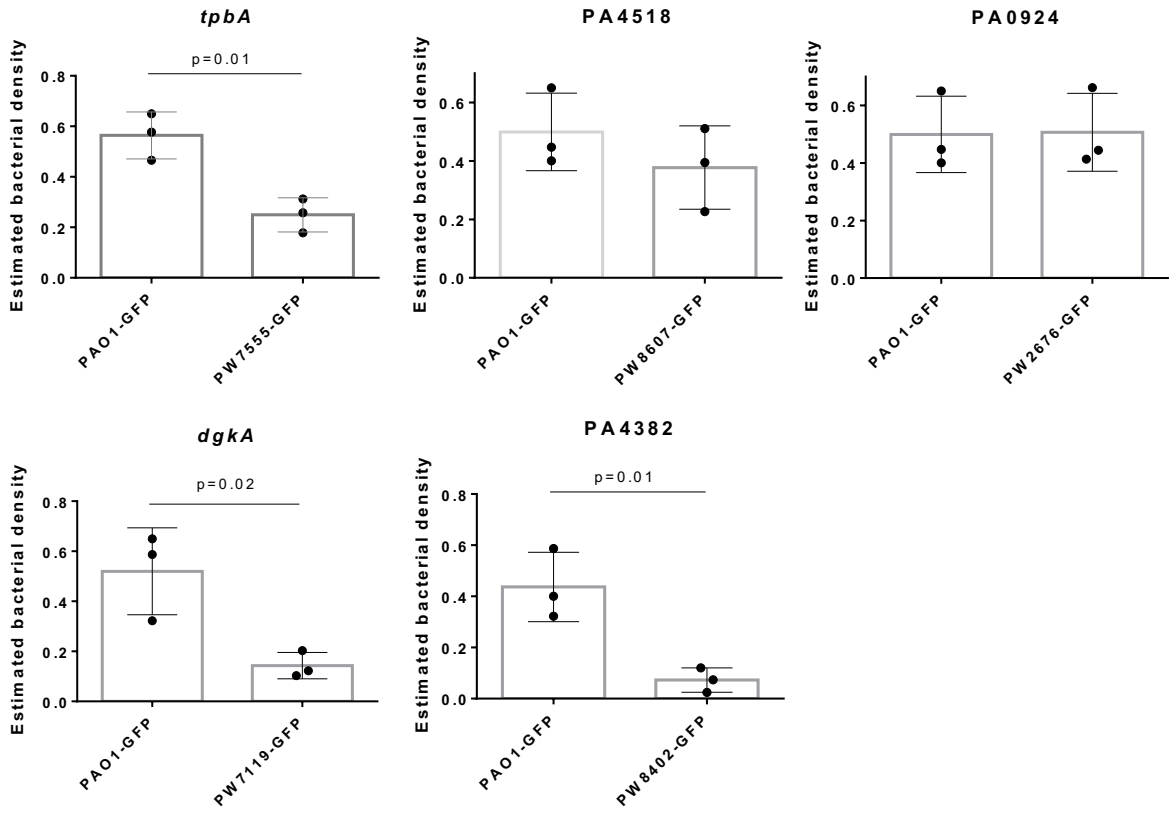

Figure 9. Mutants in a subset of genes with positively *colR*-dependent expression in the rhizosphere have defects in rhizosphere colonization. GFP-expressing PAO1 and PAO1 transposon insertion mutants from the Manoil lab two-allele library were used to perform rhizosphere colonization assays. At 5 days post-inoculation with GFP-expressing bacteria, bacterial density OD_{600} values were estimated from GFP fluorescence values using a calibration curve. Each data point represents the average of an independent experiment. P-

2.2.8 Using functional analysis of bacterial gene expression in the rhizosphere compared to minimal media to examine the rhizosphere environment.

I have shown that the response regulator ColR is required for PAO1 to colonize the Arabidopsis rhizosphere and that lack of *colR*-dependent expression of *tpbA*, *dgkA*, and PA4382 contribute to the colonization defect of the PAO1 Δ*colR* mutant. Why ColR is necessary for rhizosphere colonization is still unclear. I further investigated possible components of the rhizosphere environment that ColR may be required to protect against. To infer characteristics of

the rhizosphere environment, I examined the functional categories of genes differentially expressed between the rhizosphere and the minimal media condition in wildtype PAO1 using the RNA-seq data set.

GO enrichment analysis of differentially expressed genes in PAO1 in the rhizosphere compared to minimal media using GOfuncR revealed upregulation of catabolic processes and carbon and nitrogen metabolism (Figure 10). The increase in carbon metabolism was also found using KEGG pathway analysis in Figure 6, and as previously stated, could reflect a more diverse availability of nutrients in the rhizosphere due to the composition of MS plant growth media (85), and the secretion of root exudates by the plant (46, 99). Interestingly, all 7 genes encoding enzymes involved in the addition of L-Ara4N to lipid A in PAO1, which are the genes in the *arn* operon (*arnBCADTEF*), were up-regulated in the rhizosphere compared to in minimal media, in both PAO1 and the Δ*colR* mutant (Figure 10A). Disruption of the *arn* operon was previously found to decrease the fitness of *P. simiae* WCS417 in the rhizosphere, suggesting that this modification may be important for *P. aeruginosa* PAO1 colonization of the rhizosphere (51).

Biological processes enriched in the genes with decreased expression in the rhizosphere relative to M9 include those related to biosynthesis of many macromolecules, activity of transport systems, and ATP synthesis (Figure 10B). Many genes that encode products that function in translation, protein secretion, and biosynthesis of cofactors (cobalamin) were also repressed in *P. aeruginosa* during infection of poplar tree roots, suggesting that these are general bacterial responses to the plant rhizosphere (21).

Biological processes enriched in the genes that are down-regulated in the rhizosphere relative to M9 were involved in metal transport and iron acquisition including biosynthesis of pyoverdine (Figure 10B). Pyoverdines are fluorescent siderophores secreted by *Pseudomonas* for

iron acquisition, and their production is negatively correlated with iron availability (104). Decreased pyoverdine biosynthesis is likely caused by higher content of iron and other transition metals in MS media relative to M9 minimal media. Metals Fe^{2+}, Mn^{2+}, Co^{2+}, Cu^{2+}, and Zn^{2+} are present as micronutrients in MS media, whereas M9 minimal media only contains trace amounts of these metals (85).

Interestingly, many of the biological processes enriched in the genes down-regulated in the rhizosphere relative to M9 also require ATP. These include the biosynthetic pathways, protein secretion by the type VI secretion system (105), amino acid import (106), and translation. This suggests decreased utilization of ATP in the rhizosphere compared to M9. Lower expression of genes with products involved in ATP synthesis coupled proton transport also indicates decreased ATP synthesis. Decreased ATP synthesis and utilization could indicate that PAO1 has a slower growth rate in the rhizosphere compared to M9.

Lower ATP synthesis-dependent proton transport could also reflect growth at lower pH, where the import of extracellular and periplasmic protons may be less favourable for intracellular pH homeostasis (107, 108). The rhizosphere is often acidic and has lower pH than the surrounding soil (109). Plants also prefer to grow in slightly acidic conditions, with plant culturing media generally ranging in pH from 5.2 to 5.8 (110). The MS plant culturing media used in this study were adjusted to pH 5.8 (85), whereas the M9 minimal used as the RNA-seq control media is buffered at a pH of approximately 7. Recently, certain bacteria including *P. aeruginosa* were found to further acidify the rhizosphere to suppress aspects of plant pattern-triggered immunity (PTI) (79). Based on these enriched GO terms in the rhizosphere, I

investigated the possible contributions of transition metal toxicity and acidic pH on the growth of the Δ*colR* mutant.

2.2.9 ColR is required for tolerance to the transition metals iron, zinc, and manganese

GO enrichment analysis of gene expression in the rhizosphere compared to M9 revealed

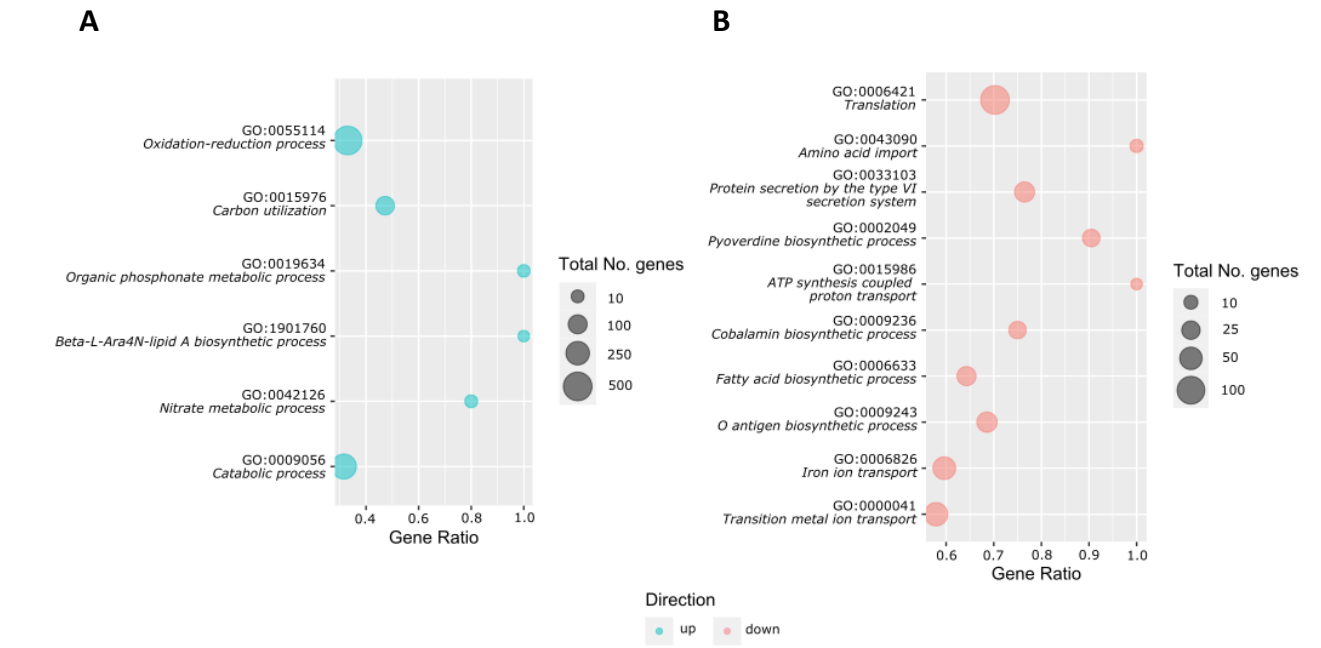

Figure 10. Changes in functional gene expression in the rhizosphere compared to minimal media. (A) Significantly enriched biological process GO terms assigned to up-regulated genes (+1.5-fold change, padj ≤ 0.05) and **(B)** select enriched biological process GO terms assigned to down-regulated genes (-1.5-fold change, padj ≤ 0.05) in PAO1 in the rhizosphere compared to minimal media. The x-axis (Gene Ratio) represents the ratio of genes annotated to a given term to the total number of genes annotated to the term in the PAO1 genome. Size of the circles corresponds to the total number of genes annotated to the term in the PAO1 genome. Biological process GO terms were obtained using GOfuncR, with FWER (family-wise error rate) ≤ 0.1 and refined p-value ≤ 0.005.

lower expression of many genes involved in metal uptake (Figure 10B). In addition, genes encoding transition ion transporters for manganese (*mntP*), iron (*fecA*), and copper (*copA1*) were dysregulated in the Δ*colR* mutant compared to wildtype PAO1 (Table 1, Figure 6). Because ColRS is required for heavy metal tolerance in *P. putida* (64), this raised the question of whether

sensitivity to the metals in the rhizosphere causes or exacerbates the rhizosphere colonization defect of the PAO1 Δ*colR* mutant.

Table 3. MIC of zinc, iron, manganese, and copper to PAO1 and PAO1 Δ*colR*. Bacterial cultures were added to a 2-fold dilution series of metals in LB. Cultures were incubated for 24h at 37˚C before observing the bacterial growth and estimating the MIC. MIC assays were repeated three times with two technical replicates. A range of MIC is shown if different MIC values were observed between replicates.

Strain	$ZnSO_4$ (mM)	$FeSO_4$ (mM)	$MnSO_4$ (mM)	$CuSO_4$ (mM)
PAO1	10	5	10	10
PAO1 Δ*colR*	5	1.25-2.5	5-10	10

To confirm the increased sensitivity of the Δ*colR* mutant towards the metals iron, zinc, manganese, and copper, I determined the minimal inhibitory concentration (MIC) of these metals in PAO1 and the Δ*colR* mutant, where the MIC is the lowest metal concentration with greater than 50% reduction in bacterial growth. I found that similar to *P. putida*, the *P. aeruginosa* PAO1 Δ*colR* mutant has lower tolerance to $ZnSO_4$ and $FeSO_4$, slightly lower tolerance to $MnSO_4$, and no change in the MIC for $CuSO_4$ (Table 3). These data indicate that *P. aeruginosa colR* is required for tolerance to some, but not all transition metals.

Using metal concentrations below the MIC in *P. aeruginosa* PAO1 Δ*colR*, I performed growth curves with PAO1 and the Δ*colR* mutant (Figure 11). I used 3 mM $CuSO_4$ even though the MIC for $CuSO_4$ for both PAO1 and PAO1 Δ*colR* was 10 mM, because neither strain showed detectable growth in ≥ 5 mM $CuSO_4$ over 24 h (data not shown). Quantification of bacterial doubling time during exponential phase and length of the lag phase are shown in Table 4. PAO1 Δ*colR* had both significantly slower doubling times, and significantly longer lag phases than PAO1 in 3 mM $ZnSO_4$, 1 mM $FeSO_4$, and 3 mM $MnSO_4$, but no significant difference during growth in 3 mM $CuSO_4$, as suggested by the MIC assay. Notably, PAO1 Δ*colR* took approximately ten times longer to reach exponential growth than PAO1 in 1 mM $FeSO_4$. This

confirms that ColR is required for tolerance to zinc, iron, and manganese, but not copper, in *P. aeruginosa*.

Though the PAO1 Δ*colR* mutant grows poorly compared to PAO1 in the presence of millimolar concentrations of metals, the metal concentrations used for the growth curves were much higher than concentrations present in ½X MS media, which are in the micromolar range (85). As bacteria were inoculated into plant wells 2 days after media change to ½X MS, metal concentrations are also likely to be lower in the rhizosphere than in the starting culture media. Plants take up transition metals as essential micronutrients (111), and many root exudate components including organic acids and amino acids have metal chelating activities (112). Taken together, we speculated that metal toxicity was likely not the main contributor to the growth defect of the Δ*colR* mutant in the rhizosphere.

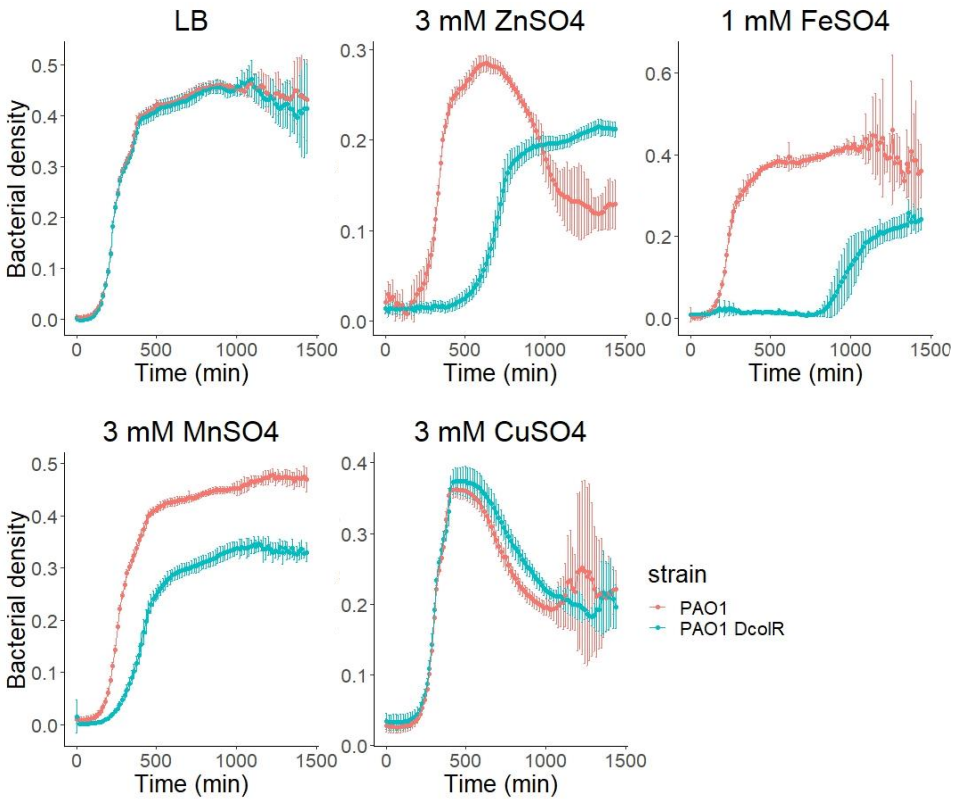

Figure 11. The *P. aeruginosa* PAO1 Δ*colR* mutant has increased sensitivity to iron, zinc, manganese, but not copper. Growth curves of PAO1 and the Δ*colR* mutant were conducted in LB liquid media with the addition of the indicated concentrations of $FeSO_4$, $ZnSO_4$, $MnSO_4$, or $CuSO_4$. Cultures were grown and OD_{600} was measured every 15 min in 96-well plates in a shaking plate reader at 37˚C for 24 h. Growth curves were repeated at least three times with similar results. Data from individual experimental replicates are shown with averages and standard deviations of 6 technical replicates per time point.

Table 4. Quantification of wildtype *P. aeruginosa* PAO1 and the PAO1 Δ*colR* mutant doubling time and duration of lag phase in transition metals. Data points used to calculate doubling time were based on growth during exponential stage, from the experiments visualized in Figure 11 (See Methods for details). Data are the average ± standard deviation of three replicates.

	Doubling time during exponential growth (min)		Start of exponential growth (min)	
Media	PAO1	PAO1 Δ*colR*	PAO1	PAO1 Δ*colR*
LB	29.11 ± 4.3	27.1 ± 4.0	95.0 ± 8.7	95.0 ± 8.7
1 mM $FeSO_4$	29.3 ± 2.3	40.4 ± 5.2*	90.0 ± 0.0	925.0 ± 173.9*
3 mM $ZnSO_4$	43.5 ± 10.7	97.7 ± 22.9*	195.9 ± 26.0	605.0 ± 239.2*
3 mM $MnSO_4$	38.6 ± 6.1	65.3 ± 4.8*	90.0 ± 26.0	245.0 ± 56.8*
3 mM $CuSO_4$	40.0 ± 5.3	41.5 ± 7.9	175.0 ± 31.2	175.0 ± 31.2

* significantly different from PAO1 ($p \leq 0.05$) by pairwise t-test

2.2.10 *P. aeruginosa* PAO1 ColR is required for adaptation to low pH.

To test whether low pH affects the growth of the Δ*colR* mutant, growth curves with wildtype PAO1 or the Δ*colR* mutant were performed in ½X MS media supplemented with either equimolar succinate or L-gln as a carbon source, and adjusted to a pH of 5, 6, or 7 (Figure 12). At pH 7 growth of the Δ*colR* mutant was indistinguishable from that of PAO1. At pH 5, however, there was little to no detectable growth of PAO1 Δ*colR* in ½X MS with neither L-gln nor succinate, whereas PAO1 entered exponential phase after an average of 60.9 min in L-gln and 42.4 min in succinate. The effect of pH on growth of the Δ*colR* mutant also depended on the carbon source provided. At pH 6 with L-gln, PAO1 Δ*colR* growth was not significantly different than PAO1, whereas at pH 6 with succinate, PAO1 Δ*colR* had a longer lag phase by an average of 370 min (Table 5), in addition to lower peak bacterial density than PAO1 (Figure 12). Quantification of bacterial doubling time during exponential phase, and time of the start of exponential phase are shown in Table 5. These data indicate that ColR is required for *P. aeruginosa* in growth at low pH, which has not been previously described. These results strongly suggests that low pH of the rhizosphere is one of the factors inhibiting the growth of the *P. aeruginosa* PAO1 Δ*colR* mutant.

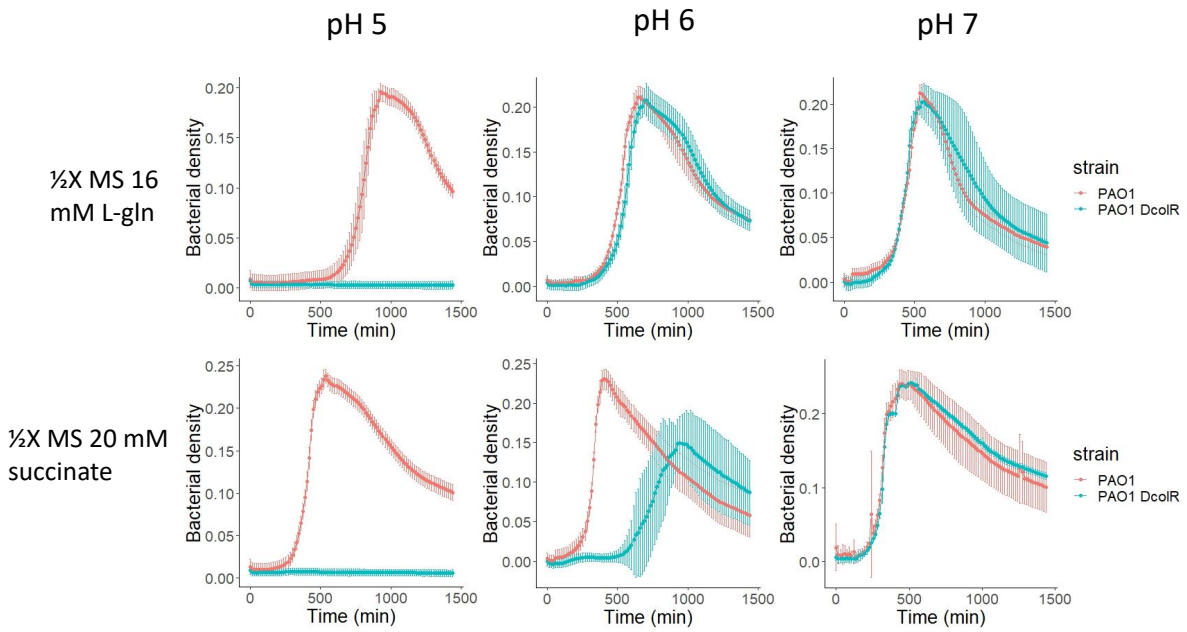

Figure 12. The Δ*colR* mutant has increased sensitivity to low pH. Growth curves of PAO1 and the Δ*colR* mutant in ½X MS media supplemented with 16 mM L-gln or 20 mM succinate at pH 5, 6, and 7. Growth curves were performed at least three times with similar results. Single experimental replicates are shown with averages and standard deviations of 6 technical replicates per time point.

Table 5. Quantification of *P. aeruginosa* PAO1 and PAO1 Δ*colR* doubling time and duration of lag phase in ½X MS media at varying pH. Data points used to calculate doubling time were based on growth during exponential stage, from the experiments visualized in Figure 12 (See Methods for details). Data are the average ± standard deviation of three replicates.

		Generation time during exponential growth (min)		Start of exponential growth (min)	
Media	pH	PAO1	PAO1 Δ*colR*	PAO1	PAO1 Δ*colR*
½X MS 16 mM L-gln	5	60.9 ± 10.2	N/A	590.0 ± 60.6	N/A
	6	62.1 ± 6.5	65.7 ± 11.0	395.0 ± 95.3	355.0 ± 75.5
	7	51.4 ± 7.4	46.7 ± 1.8	295.0 ± 22.9	295.0 ± 22.9
½X MS 20 mM succinate	5	42.4 ± 10.8	N/A	225.0 ± 15.0	N/A
	6	36.9 ± 6.7	50.1 ± 9.7	180.0 ± 39.7	550.0 ± 56.8*
	7	46.4 ± 2.9	47.3 ± 4.4	155.0 ± 17.3	170.0 ± 8.7

* significantly different from PAO1 ($p \leq 0.05$) by pairwise t-test

N/A – Growth curve did not consistently reach exponential phase before end of 24h period.

Chapter 3: Discussion

3.1 ColRS is a conserved regulator of rhizosphere colonization factors in *Pseudomonas* spp.

I found that like in *P. fluorescens* and *P. simiae* (50, 51), *P. aeruginosa colRS* is required for colonization of the Arabidopsis rhizosphere (Figure 2; 50). This suggests that ColRS regulates conserved genes required for growth of diverse *Pseudomonas* spp. in the plant rhizosphere. Therefore, studying ColRS regulation in *P. aeruginosa* PAO1, a model *Pseudomonas* strain with a well-annotated genome, has the potential to identify rhizosphere colonization factors that are conserved in beneficial plant-associated *Pseudomonas*. My RNA-seq results, and previous studies, indicate that *dgkA* and the PAP2-encoding PA4382 are *colR*-dependent in both *P. aeruginosa* (Figure 7) and *P. putida* (63), and I found that *dgkA* and PA4382 are required for *P. aeruginosa* rhizosphere colonization (Figure 9). Since ColRS is a conserved rhizosphere colonization factor across *Pseudomonas,* both *dgkA* and PA4382 orthologs could function in rhizosphere colonization across diverse *Pseudomonas* spp.

3.2 The ColRS regulon is partially conserved between *Pseudomonas* spp.

A high degree of sequence similarity between *P. putida* ColR, *P. fluorescens* ColR, and *P. aeruginosa* ColR (Figure 1), and similar growth defects of the *colR* mutant in the rhizosphere, iron, zinc, and manganese (Figure 2 and 11) strongly suggests that ColR regulates similar genes and processes across *Pseudomonas* spp. (50, 64). Several *colR*-dependent genes in *P. aeruginosa* identified by my RNA-seq analysis were previously found to be ColR-regulated in *P. putida* (63, 64), which serves as a validation for my RNA-seq experiment and indicates conservation of the ColR regulon. *P. aeruginosa dgkA*, PA4382 and their orthologs in *P. putida* are examples of genes that are *colR*-dependent in both organisms (Figure 7; 63). A *colR*-dependent operon in *P.*

aeruginosa, *warAB* (Figure 7), is also ColR-regulated in *P. fluorescens* and *P. putida* (53, 63). PA4517 encodes a pEtN transferase in *P. aeruginosa* PAO1 and is *colR*-dependent in the rhizosphere (Figure 7); its ortholog in *P. putida*, *cptA*, is ColR-regulated in high concentrations of zinc (64).

The expression of most of the *colR*-dependent genes in *P. aeruginosa* identified by RNA-seq have not been previously shown to be *colR*-dependent in *P. putida* or *P. fluorescens*. These include *tpbA*, encoding a protein tyrosine phosphatase, *mntP*, encoding a manganese efflux pump, and the *agtABCD* operon, encoding a polyamine ABC transporter (Figure 7, Table 2). BLAST search results of the *P. aeruginosa colR*-dependent genes against *P. putida* KT2440, identified *P. aeruginosa* genes that do not have an obvious homolog (below 30% identity, or no significant similarity found) in *P. putida*, such as *tpbA* and *mntP*. Genes in the *agtABCD* operon are conserved in *P. putida* (83-90% identity) but were not predicted to be ColR-regulated. There are also ColR-regulated genes in *P. putida* that did not show *colR*-dependence in my RNA-seq analysis. These include *oprQ* encoding an outer membrane protein and *pagL,* encoding a lipid 3-*O*-deacylase, which are directly repressed by ColR in *P. putida* (63). It is possible that these ColR-regulated genes are not *colR*-dependent in the rhizosphere, or the ColRS regulon has diverged between *Pseudomonas* spp.

RNA-seq analysis of *P. aeruginosa* PAO1 and PAO1 Δ*colR* gene expression in the rhizosphere identified *colR*-dependent genes in *P. aeruginosa* that were previously identified in *P. putida*, and genes that may be unique to the ColR-regulon of the different species. Collectively, these results suggest a partial conservation of the ColR-regulon across *Pseudomonas* spp.

3.3 ColR induces the expression of multiple LPS modification enzymes in rhizosphere-growing *P. aeruginosa*.

Consistent with the hypothesis that ColRS regulates outer membrane integrity, I found *colR*-dependent expression of several genes involved in LPS modification. My RNA-seq analysis found that three genes encoding predicted pEtN transferases in PAO1, *eptA*, PA3310, and PA4517, had a *colR*-dependent increase in expression in the rhizosphere (Figure 7, Table 2). EptA is the only predicted pEtN transferase among the three gene products that targets the lipid A of LPS (70). PA4517 likely targets the LPS core sugars, as it has 63% amino acid sequence identity to *Salmonella enterica* CptA (96). PA3310 could potentially target flagella and pili, which are other targets of pEtN modification found in Gram-negative bacteria (113, 114). From the characterized and predicted functions of the enzymes encoded by *eptA* and PA4517, ColR likely regulates the expression of genes required for pEtN transferase modification of both the lipid A and core portions of LPS.

I also found that the *warAB* operon has *colR*-dependent induction in the rhizosphere (Figure 7) (57). *P. aeruginosa* WarA is a c-di-GMP-binding methyltransferase and WarB is a putative LPS kinase (57). WarA and WarB likely function together to phosphorylate and methylate the terminal reducing end of a growing O-antigen chain on LPS to terminate its extension (57, 115). Deletion of *warA* in *P. aeruginosa* increased the average O-antigen chain length, while overexpression of *warA* decreased the average O-antigen chain length (57). Decreased expression of *warAB* in PAO1 Δ*colR* compared to PAO1 in the rhizosphere suggests that PAO1 Δ*colR* may have LPS with longer O-antigens.

Though differences in gene expression suggests that the PAO1 Δ*colR* outer membrane has an altered LPS profile, whether and how these LPS modifications contribute to *P. aeruginosa*

fitness in the rhizosphere is unclear. Nuclear magnetic resonance (NMR) or matrix-assisted laser desorption/ionization-time of flight (MALDI-TOF) mass spectrometry analysis of LPS from wildtype *P. aeruginosa* and the Δ*colR* mutant should provide direct evidence of changes to LPS composition (96). Though single transposon mutants in *eptA*, PA3310, PA4517, or *warA* did not result in rhizosphere colonization defects (Figure 4B, Table 2), this could be explained by functional redundancy within the ColR-regulon. In *P. putida*, deletion of 3 or more ColR-regulated loci was required to have a significant impact on zinc sensitivity, suggesting that the loss of one or two ColR-regulated genes could be compensated for by other genes in the regulon (64). In *Haemophilus ducreyi*, another bacteria with three predicted pEtN transferases, only deletion of all three genes encoding predicted pEtN transferases resulted in a significant decrease in resistance to human defensins (116). Therefore, I speculate that the LPS modification enzymes regulated by ColR could have functional redundancy in their contribution to PAO1 fitness in the rhizosphere.

3.4 ColR and heavy metal tolerance

Heavy metal tolerance is a ColRS-regulated phenotype that has been extensively studied in *P. putida*. Mutation in either *colR* or *colS* decreased the tolerance of *P. putida* to growth on media with high levels of select heavy metals: zinc, iron, manganese, and cadmium, but not cobalt, copper, or nickel (64). Consistent with this, I found that loss of *colR* also negatively impacts growth of *P. aeruginosa* in media containing high levels of zinc, iron, and manganese, but not copper (Figure 11). I found that high levels of $ZnSO_4$, $FeSO_4$, and $MnSO_4$ decrease the growth rate and increase the duration of lag phase of PAO1 Δ*colR* relative to PAO1 (Table 4). The increased lag phase of PAO1 Δ*colR* in $ZnSO_4$, $FeSO_4$, and $MnSO_4$ likely indicate slower

adaptation to growth at high concentrations of these metals through ColRS-independent mechanisms.

ColS in *P. putida* has been hypothesized to directly bind and sense the presence of Zn^{2+} and Fe^{3+} ions through a periplasmic ExxE motif (Figure 1) (64). Though I used Fe^{2+} instead of Fe^{3+} in $FeSO_4$, Fe^{2+} quickly oxidizes to Fe^{3+} in the media (64). I observed that PAO1 Δ*colR* exhibited biphasic growth in $FeSO_4$, with a short initial exponential growth phase followed by a long lag, and a second exponential growth phase at approximately 925 min (Figure 11). I speculate that PAO1 Δ*colR* was initially not impaired in growth in Fe^{2+}, but was unable to quickly adapt after oxidation of Fe^{2+} to Fe^{3+}.

It is intriguing that PAO1 Δ*colR* had a pronounced growth defect in high levels of $FeSO_4$ and $ZnSO_4$ but not in high levels of $CuSO_4$ (Figure 11). Iron, zinc, and copper are essential micronutrients, however iron is required at higher amounts to support bacterial growth, and competition for iron is a frequent battle at the host-pathogen interface (117). Proteins that require iron as cofactors are involved in essential intracellular processes including respiration and nucleotide biosynthesis (117). Excess free iron is toxic to cells however, mainly through the Fenton reaction, in which Fe^{2+} reacts with hydrogen peroxide (H_2O_2) to generate damaging reactive oxygen species (ROS) (118). Because iron is both essential and toxic, *P. aeruginosa* has extensive methods for iron acquisition, sequestering, and detoxification (104, 119). In contrast, copper is a general antimicrobial agent is used in healthcare settings to reduce bacterial contamination (120). Cu^{2+} has the highest metal complex stability out of the divalent metals in the first transition metal row of the periodic table (121), which means that free copper in the cytoplasm has the highest tendency to replace metal cofactors in metalloproteins to cause mismetallation. Therefore, the growth defects of PAO1 Δ*colR* in $FeSO_4$ and $ZnSO_4$ were likely

not due to a general increase in membrane permeability towards divalent cationic transition metals; if this were the case, PAO1 Δ*colR* should also have decreased tolerance to $CuSO_4$. I speculate that PAO1 Δ*colR* may be unable to suppress the uptake of, or to sequester or export specific metal ions including Zn^{2+} and Fe^{3+}. Higher expression of *fecA* in PAO1 Δ*colR* relative to wildtype PAO1 (Table 1), a gene involved in citrate-mediated Fe^{3+} import (122, 123), could potentially contribute to the lower tolerance of PAO1 Δ*colR* to Fe^{3+}.

3.5 Combination of low pH and soluble metals as abiotic stresses in the rhizosphere.

I have shown that the *P. aeruginosa colR* mutant has a growth defect at low pH. At pH 5, there was no growth of PAO1 Δ*colR* mutant, while at pH 7 the growth of PAO1 Δ*colR* was similar to wildtype PAO1 (Figure 12). How ColRS protects *P. aeruginosa* from low pH requires further investigation. Two-component systems have been shown to sense and respond to acidic pH in other bacteria. In *Salmonella,* the two-component system PhoPQ is activated by low pH and induces a PhoPQ-dependent acid tolerance response (124). The sensor PhoQ may undergo a conformational change after exposure to pH 5.5 due to protonation of histidine residues in the periplasmic or the cytoplasmic domain (55, 125). Another two-component system, CpxRA, regulates an acid tolerance response in *E. coli* (108). The sensor, CpxA, is also capable of sensing low pH through protonation of periplasmic histidine residues (108). PhoPQ regulates many lipid A modification enzymes (55), and CpxAR can respond to cell envelop stress by regulating outer membrane porins OmpC and OmpF, and increasing production of unsaturated fatty acids (108, 126), in their respective organisms. Given that ColR regulates several LPS modification genes, it is possible that ColRS also contributes to acid tolerance by regulating outer membrane composition.

Because solubility of metals is dependent on pH (109, 127, 128), pH stress may also increase soluble zinc, iron, and manganese. Low pH could directly function to inhibit the growth of PAO1 Δ*colR* in the rhizosphere, indirectly through increasing the concentration of soluble transition metals in the rhizosphere, or both. Although I found that the $FeSO_4$ and $ZnSO_4$ MIC of PAO1 Δ*colR* in LB were much higher than the concentrations present in ½X MS media (Table 3; 85), ½X MS is more acidic than LB. Lower pH of the rhizosphere may decrease the metal MIC of PAO1 Δ*colR*, and combined with the presence of multiple transition metals in the plant culture medium, could serve to inhibit the growth of PAO1 Δ*colR* in the rhizosphere.

3.6 Conclusion and future directions

In summary, I found that *P. aeruginosa colR* is required for Arabidopsis rhizosphere colonization and *in vitro* tolerance to metals and low pH. Currently, it is not known which *colR*-dependent genes are responsible for conferring tolerance to metals or low pH. To dissect the genetic basis of the *colR*-dependent tolerance to zinc, iron, manganese, and to low pH, the transposon insertion mutants in *colR*-dependent genes PAO1 two-allele library could be tested for impaired growth in high concentrations of metals or low pH. Because of the possible functional redundancy in the ColR-regulon as previously described, mutations in multiple ColR-induced genes may be required to see a significant defect in the *in vitro* phenotypes. Identification of mutants that are impaired for growth in both the rhizosphere and in media with high metal content or low pH would further strengthen the hypothesis that these abiotic stresses inhibit the growth of PAO1 Δ*colR* in the rhizosphere. It would also be interesting if any *colR*-dependent genes required for rhizosphere colonization, such as *tpbA*, *dgkA*, and PA4382, were

not required for growth in high concentration of metals or in low pH, as this would suggest that ColR is required for adaptation to multiple distinct stresses in the rhizosphere.

Lastly, we showed that *colR* in a chronic infection isolate LESB58 positively influences virulence in a mouse abscess model (Figure 3). We speculate that the reduced abscess area and tissue necrosis could indicate that *colR* is involved in regulating virulence factors, or factors that elicit murine innate immunity (17). ColR-dependent genes in the rhizosphere are also virulence factor candidates in a mouse model. Characterization of abscess formation by deletion mutants in *colR*-dependent genes could lead to the discovery of ColRS-regulated multi-host association factors in *P. aeruginosa*.

References

1. Rice LB. 2008. Federal Funding for the Study of Antimicrobial Resistance in Nosocomial Pathogens: No ESKAPE. J Infect Dis 197:1079–1081.
2. De Oliveira DMP, Forde BM, Kidd TJ, Harris PNA, Schembri MA, Beatson SA, Paterson DL, Walker MJ. 2020. Antimicrobial resistance in ESKAPE pathogens. Clin Microbiol Rev 33:e00181-19.
3. Holder IA. 1993. *P. aeruginosa* Burn Infections: Pathogenesis and Treatment, p. 275–295. *In* Pseudomonas aeruginosa as an Opportunistic Pathogen. Springer, Boston, MA.
4. Serra R, Grande R, Butrico L, Rossi A, Settimio UF, Caroleo B, Amato B, Gallelli L, De Franciscis S. 2015. Chronic wound infections: The role of *Pseudomonas aeruginosa* and *Staphylococcus aureus*. Expert Rev Anti Infect Ther 13:605–613.
5. Lyczak JB, Cannon CL, Pier GB. 2002. Lung infections associated with cystic fibrosis. Clin Microbiol Rev 15:194–222.
6. Römling U, Balsalobre C. 2012. Biofilm infections, their resilience to therapy and innovative treatment strategies. J Intern Med 272:541–561.
7. Heacock-Kang Y, Sun Z, Zarzycki-Siek J, McMillan IA, Norris MH, Bluhm AP, Cabanas D, Fogen D, Vo H, Donachie SP, Borlee BR, Sibley CD, Lewenza S, Schurr MJ, Schweizer HP, Hoang TT. 2017. Spatial transcriptomes within the *Pseudomonas aeruginosa* biofilm architecture. Mol Microbiol 106:976–985.
8. Breidenstein EBM, de la Fuente-Núñez C, Hancock REW. 2011. *Pseudomonas aeruginosa*: All roads lead to resistance. Trends Microbiol 19:419–426.
9. Stieritz DD, Holder IA. 1975. Experimental studies of the pathogenesis of infections due to *Pseudomonas aeruginosa*: description of a burned mouse model. J Infect Dis 31:688–692.
10. Plotnikova JM, Rahme LG, Ausubel FM. 2000. Pathogenesis of the human opportunistic pathogen *Pseudomonas aeruginosa* PA14 in Arabidopsis. Plant Physiol 124:1766–74.
11. Walker TS, Bais HP, Déziel E, Schweizer HP, Rahme LG, Fall R, Vivanco JM. 2004. *Pseudomonas aeruginosa*-plant root interactions. Pathogenicity, biofilm formation, and root exudation. Plant Physiol 134:320–31.
12. Mahajan-Miklos S, Tan MW, Rahme LG, Ausubel FM. 1999. Molecular mechanisms of bacterial virulence elucidated using a *Pseudomonas aeruginosa-Caenorhabditis elegans* pathogenesis model. Cell 96:47–56.
13. Clatworthy AE, Lee JSW, Leibman M, Kostun Z, Davidson AJ, Hung DT. 2009. *Pseudomonas aeruginosa* infection of zebrafish involves both host and pathogen determinants. Infect Immun 77:1293–1303.
14. Stover CK, Pham XQ, Erwin AL, Mizoguchi SD, Warrener P, Hickey MJ, Brinkman FSL, Hufnagle WO, Kowalik DJ, Lagrou M, Garber RL, Goltry L, Tolentino E, Westbrock-Wadman S, Yuan Y, Brody LL, Coulter SN, Folger KR, Kas A, Larbig K, Lim R, Smith K, Spencer D, Wong GK-S, Wu Z, Paulsen IT, Reizer J, Saier MH, Hancock REW, Lory S, Olson M V. 2000. Complete genome sequence of *Pseudomonas aeruginosa* PAO1, an opportunistic pathogen. Nature 406:959–964.
15. Ezeador CO, Ejikeugwu PC, Ushie SN, Agbakoba NR. 2020. Isolation, Identification And Prevalence Of *Pseudomonas aeruginosa* Isolates From Clinical And Environmental Sources In Onitsha Metropolis, Anambra State. Eur J Med Heal Sci 2.
16. Johansen HK, Høiby N. 1999. Rat Model of Chronic *Pseudomonas aeruginosa* Lung

Infection, p. 517–526. *In* Handbook of Animal Models of Infection. Elsevier.
17. Pletzer D, Mansour SC, Wuerth K, Rahanjam N, Hancock REW. 2017. New Mouse Model for Chronic Infections by Gram-Negative Bacteria Enabling the Study of Anti-Infective Efficacy and Host-Microbe Interactions. MBio 8:e00140-17.
18. Cheng K, Smyth RL, Govan JRW, Doherty C, Winstanley C, Denning N, Heaf DP, Van Saene H, Hart CA. 1996. Spread of β-lactam-resistant *Pseudomonas aeruginosa* in a cystic fibrosis clinic. Lancet 348:639–642.
19. Erickson DL, Lines JL, Pesci EC, Venturi V, Storey DG. 2004. *Pseudomonas aeruginosa relA* contributes to virulence in *Drosophila melanogaster*. Infect Immun 72:5638–5645.
20. Jander G, Rahme LG, Ausubel FM. 2000. Positive correlation between virulence of Pseudomonas aeruginosa mutants in mice and insects. J Bacteriol 182:3843–5.
21. Attila C, Ueda A, Cirillo SLG, Cirillo JD, Chen W, Wood TK. 2008. *Pseudomonas aeruginosa* PAO1 virulence factors and poplar tree response in the rhizosphere. Microb Biotechnol 1:17–29.
22. Rahme LG, Ausubel FM, Cao H, Drenkard E, Goumnerov BC, Lau GW, Mahajan-Miklos S, Plotnikova J, Tan MW, Tsongalis J, Walendziewicz CL, Tompkins RG. 2000. Plants and animals share functionally common bacterial virulence factors. Proc Natl Acad Sci U S A 97:8815–8821.
23. Garvis S, Munder A, Ball G, de Bentzmann S, Wiehlmann L, Ewbank JJ, Tümmler B, Filloux A. 2009. *Caenorhabditis elegans* semi-automated liquid screen reveals a specialized role for the chemotaxis gene *cheB2* in *Pseudomonas aeruginosa* virulence. PLoS Pathog 5:e1000540.
24. Rahme LG, Stevens EJ, Wolfort SF, Shao J, Tompkins RG, Ausubel FM. 1995. Common virulence factors for bacterial pathogenicity in plants and animals. Science (80-) 268:1899–1902.
25. Tan MW, Mahajan-Miklos S, Ausubel FM. 1999. Killing of *Caenorhabditis elegans* by *Pseudomonas aeruginosa* used to model mammalian bacterial pathogenesis. Proc Natl Acad Sci U S A 96:715–720.
26. Kirienko N V., Ausubel FM, Ruvkun G. 2015. Mitophagy confers resistance to siderophore-mediated killing by *Pseudomonas aeruginosa*. Proc Natl Acad Sci U S A 112:1821–1826.
27. Beeton ML, Alves DR, Enright MC, Jenkins ATA. 2015. Assessing phage therapy against *Pseudomonas aeruginosa* using a *Galleria mellonella* infection model. Int J Antimicrob Agents 46:196–200.
28. Pires DP, Vilas Boas D, Sillankorva S, Azeredo J. 2015. Phage Therapy: a Step Forward in the Treatment of *Pseudomonas aeruginosa* Infections. J Virol 89:7449–7456.
29. Jeon J, Yong D. 2019. Two novel bacteriophages improve survival in Galleria mellonella infection and mouse acute pneumonia models infected with extensively drug-resistant Pseudomonas aeruginosa. Appl Environ Microbiol 85.
30. Cook J, Douglas GM, Zhang J, Glick BR, Langille MGI, Liu K-H, Cheng Z. 2020. Transcriptomic profiling of *Brassica napus* responses to *Pseudomonas aeruginosa*. Innate Immun 175342592098051.
31. Koornneef M, Meinke D. 2010. The development of Arabidopsis as a model plant. Plant J 61:909–921.
32. Rahme LG, Tan MW, Le L, Wong SM, Tompkins RG, Calderwood SB, Ausubel FM. 1997. Use of model plant hosts to identify *Pseudomonas aeruginosa* virulence factors.

Proc Natl Acad Sci U S A 94:13245–13250.
33. Green SK, Schroth MN, Cho JJ, Kominos SD, Vitanza-Jack VB. 1974. Agricultural Plants and Soil as a Reservoir for *Pseudomonas aeruginosa*. Appl Environ Microbiol 28.
34. Kominos SD, Copeland CE, Grosiak B, Postic B. 1972. Introduction of *Pseudomonas aeruginosa* into a hospital via vegetables. Appl Microbiol 24:567–570.
35. Cho JJ. 1975. Ornamental Plants as Carriers of *Pseudomonas aeruginosa*. Phytopathology 65:425.
36. Anjaiah V, Cornelis P, Koedam N. 2003. Effect of genotype and root colonization in biological control of fusarium wilts in pigeonpea and chickpea by *Pseudomonas aeruginosa* PNA1. Can J Microbiol 49:85–91.
37. Yasmin S, Hafeez FY, Mirza MS, Rasul M, Arshad HMI, Zubair M, Iqbal M. 2017. Biocontrol of Bacterial Leaf Blight of rice and profiling of secondary metabolites produced by rhizospheric *Pseudomonas aeruginosa* BRp3. Front Microbiol 8.
38. Troxler J, Azelvandre P, Zala M, Défago G, Haas D. 1997. Conjugative transfer of chromosomal genes between fluorescent pseudomonads in the rhizosphere of wheat. Appl Environ Microbiol 63:213–219.
39. Mark GL, Dow JM, Kiely PD, Higgins H, Haynes J, Baysse C, Abbas A, Foley T, Franks A, Morrissey J, O'Gara F. 2005. Transcriptome profiling of bacterial responses to root exudates identifies genes involved in microbe-plant interactions. Proc Natl Acad Sci U S A 102:17454–17459.
40. Elrod RP, Braun AC. 1942. *Pseudomonas aeruginosa*: Its Role as a Plant Pathogen. J Bacteriol 44:633–645.
41. Starkey M, Rahme LG. 2009. Modeling Pseudomonas aeruginosa pathogenesis in plant hosts. Nat Protoc 4:117–124.
42. Spago FR, Ishii Mauro CS, Oliveira AG, Beranger JPO, Cely MVT, Stanganelli MM, Simionato AS, San Martin JAB, Andrade CGTJ, Mello JCP, Andrade G. 2014. *Pseudomonas aeruginosa* produces secondary metabolites that have biological activity against plant pathogenic *Xanthomonas* species. Crop Prot 62:46–54.
43. Canarini A, Kaiser C, Merchant A, Richter A, Wanek W. 2019. Root exudation of primary metabolites: Mechanisms and their roles in plant responses to environmental stimuli. Front Plant Sci 10.
44. Tian T, Reverdy A, She Q, Sun B, Chai Y. 2020. The role of rhizodeposits in shaping rhizomicrobiome. Environ Microbiol Rep 12:160–172.
45. Baetz U, Martinoia E. 2014. Root exudates: The hidden part of plant defense. Trends Plant Sci 19:90–98.
46. Badri D V., Vivanco JM. 2009. Regulation and function of root exudates. Plant, Cell Environ 32:666–681.
47. De Weger LA, Van Der Vlugt CIM, Wijfjes AHM, Bakker PA, Schippers B, Lugtenberg B. 1987. Flagella of a plant-growth-stimulating *Pseudomonas fluorescens* strain are required for colonization of potato roots. J Bacteriol 169:2769–2773.
48. De Weert S, Vermeiren H, Mulders IHM, Kuiper I, Hendrickx N, Bloemberg G V., Vanderleyden J, De Mot R, Lugtenberg BJJ. 2002. Flagella-driven chemotaxis towards exudate components is an important trait for tomato root colonization by *Pseudomonas fluorescens*. Mol Plant-Microbe Interact 15:1173–1180.
49. Simons M, Permentier HP, De Weger LA, Wijffelman CA, Lugtenberg BJJ. 1997. Amino acid synthesis is necessary for tomato root colonization by *Pseudomonas fluorescens*

strain WCS365. Mol Plant-Microbe Interact 10:102–106.
50. Dekkers LC, Bloemendaal CJP, de Weger LA, Wijffelman CA, Spaink HP, Lugtenberg BJJ. 1998. A Two-Component System Plays an Important Role in the Root-Colonizing Ability of *Pseudomonas fluorescens* Strain WCS365. Mol Plant-Microbe Interact 11:45–56.
51. Cole BJ, Feltcher ME, Waters RJ, Wetmore KM, Mucyn TS, Ryan EM, Wang G, Ul-Hasan S, McDonald M, Yoshikuni Y, Malmstrom RR, Deutschbauer AM, Dangl JL, Visel A. 2017. Genome-wide identification of bacterial plant colonization genes. PLoS Biol 15.
52. Liu Z, Beskrovnaya P, Melnyk RA, Hossain SS, Khorasani S, O'Sullivan LR, Wiesmann CL, Bush J, Richard JD, Haney CH. 2018. A Genome-Wide Screen Identifies Genes in Rhizosphere-Associated *Pseudomonas* Required to Evade Plant Defenses. MBio 9:e00433-18.
53. De Weert S, Dekkers LC, Bitter W, Tuinman S, Wijfjes AHM, Van Boxtel R, Lugtenberg BJJ. 2006. The two-component *colR/S* system of *Pseudomonas fluorescens* WCS365 plays a role in rhizosphere competence through maintaining the structure and function of the outer membrane. FEMS Microbiol Ecol 58:205–213.
54. Trimble MJ, Mlynárčik P, Kolář M, Hancock REW. 2016. Polymyxin: Alternative mechanisms of action and resistance. Cold Spring Harb Perspect Med 6.
55. Simpson BW, Trent MS. 2019. Pushing the envelope: LPS modifications and their consequences. Nat Rev Microbiol 17:403–416.
56. Dekkers LC, Van Der Bij AJ, Mulders IHM, Phoelich CC, Wentwoord RAR, Glandorf DCM, Wijffelman CA, Lugtenberg BJJ. 1998. Role of the O-antigen of lipopolysaccharide, and possible roles of growth rate and of NADH:ubiquinone oxidoreductase (nuo) in competitive tomato root-tip colonization by *Pseudomonas fluorescens* WCS365. Mol Plant-Microbe Interact 11:763–771.
57. McCarthy RR, Mazon-Moya MJ, Moscoso JA, Hao Y, Lam JS, Bordi C, Mostowy S, Filloux A. 2017. Cyclic-di-GMP regulates lipopolysaccharide modification and contributes to *Pseudomonas aeruginosa* immune evasion. Nat Microbiol 2:17027.
58. Sonawane AM, Singh B, Röhm KH. 2006. The AauR-AauS two-component system regulates uptake and metabolism of acidic amino acids in *Pseudomonas putida*. Appl Environ Microbiol 72:6569–6577.
59. Francis VI, Stevenson EC, Porter SL. 2017. Two-component systems required for virulence in *Pseudomonas aeruginosa*. FEMS Microbiol Lett 364:104.
60. Gellatly SL, Needham B, Madera L, Trent MS, Hancock REW. 2012. The *Pseudomonas aeruginosa phoP-phoQ* two-component regulatory system is induced upon interaction with epithelial cells and controls cytotoxicity and inflammation. Infect Immun 80:3122–3131.
61. Stock AM, Robinson VL, Goudreau PN. 2000. Two-Component Signal Transduction. Annu Rev Biochem 69:183–215.
62. Capra EJ, Laub MT. 2012. Evolution of two-component signal transduction systems. Annu Rev Microbiol 66:325–347.
63. Kivistik PA, Kivi R, Kivisaar M, Hõrak R. 2009. Identification of ColR binding consensus and prediction of regulon of ColRS two-component system. BMC Mol Biol 10:46.
64. Ainsaar K, Mumm K, Ilves H, Hõrak R. 2014. The ColRS signal transduction system responds to the excess of external zinc, iron, manganese, and cadmium. BMC Microbiol 14:162.

65. Gutu AD, Sgambati N, Strasbourger P, Brannon MK, Jacobs MA, Haugen E, Kaul RK, Johansen HK, Høiby N, Moskowitz SM. 2013. Polymyxin resistance of *Pseudomonas aeruginosa phoQ* mutants is dependent on additional two-component regulatory systems. Antimicrob Agents Chemother 57:2204–2215.
66. Miller AK, Brannon MK, Stevens L, Johansen HK, Selgrade SE, Miller SI, Høiby N, Moskowitz SM. 2011. PhoQ mutations promote lipid A modification and polymyxin resistance of *Pseudomonas aeruginosa* found in colistin-treated cystic fibrosis patients. Antimicrob Agents Chemother 55:5761–5769.
67. Sciuto A Lo, Imperi F. 2018. Aminoarabinosylation of lipid a is critical for the development of colistin resistance in *Pseudomonas aeruginosa*. Antimicrob Agents Chemother 62.
68. Zhang DF, Li H, Lin XM, Wang SY, Peng XX. 2011. Characterization of outer membrane proteins of *Escherichia coli* in response to phenol stress. Curr Microbiol 62:777–783.
69. Kivistik PA, Putrins M, Püvi K, Ilves H, Kivisaar M, Hõrak R. 2006. The ColRS two-component system regulates membrane functions and protects *Pseudomonas putida* against phenol. J Bacteriol 188:8109–17.
70. Nowicki EM, O'Brien JP, Brodbelt JS, Trent MS. 2015. Extracellular zinc induces phosphoethanolamine addition to *Pseudomonas aeruginosa* lipid A via the ColRS two-component system. Mol Microbiol 97:166–78.
71. Gillet S, Lawarée E, Matroule JY. 2018. Functional Diversity of Bacterial Strategies to Cope With Metal Toxicity, p. 409–426. *In* Microbial Diversity in the Genomic Era. Academic Press.
72. McDevitt CA, Ogunniyi AD, Valkov E, Lawrence MC, Kobe B, McEwan AG, Paton JC. 2011. A molecular mechanism for bacterial susceptibility to zinc. PLoS Pathog 7.
73. Mumm K, Ainsaar K, Kasvandik S, Tenson T, Hõrak R. 2016. Responses of *Pseudomonas putida* to Zinc Excess Determined at the Proteome Level: Pathways Dependent and Independent of ColRS. J Proteome Res 15:4349–4368.
74. Yao J, Rock CO. 2013. Phosphatidic acid synthesis in bacteria. Biochim Biophys Acta - Mol Cell Biol Lipids 1831:495–502.
75. Zhang YM, Rock CO. 2008. Membrane lipid homeostasis in bacteria. Nat Rev Microbiol 6:222–233.
76. Jacobs MA, Alwood A, Thaipisuttikul I, Spencer D, Haugen E, Ernst S, Will O, Kaul R, Raymond C, Levy R, Chun-Rong L, Guenthner D, Bovee D, Olson M V., Manoil C. 2003. Comprehensive transposon mutant library of *Pseudomonas aeruginosa*. Proc Natl Acad Sci 100:14339–14344.
77. Putrinš M, Ainelo A, Ilves H, Hõrak R. 2011. The ColRS system is essential for the hunger response of glucose-growing *Pseudomonas putida*. BMC Microbiol 11:170.
78. Vivijs B, Aertsen A, Michiels CW. 2016. Identification of genes required for growth of *Escherichia coli* MG1655 at moderately low pH. Front Microbiol 7:1672.
79. Yu K, Liu Y, Tichelaar R, Savant N, Lagendijk E, van Kuijk SJL, Stringlis IA, van Dijken AJH, Pieterse CMJ, Bakker PAHM, Haney CH, Berendsen RL. 2019. Rhizosphere-Associated *Pseudomonas* Suppress Local Root Immune Responses by Gluconic Acid-Mediated Lowering of Environmental pH. Curr Biol 29:3913-3920.e4.
80. Hmelo LR, Borlee BR, Almblad H, Love ME, Randall TE, Tseng BS, Lin C, Irie Y, Storek KM, Yang JJ, Siehnel RJ, Howell PL, Singh PK, Tolker-Nielsen T, Parsek MR, Schweizer HP, Harrison JJ. 2015. Precision-engineering the *Pseudomonas aeruginosa*

genome with two-step allelic exchange. Nat Protoc 10:1820–1841.
81. Ho SN, Hunt HD, Horton RM, Pullen JK, Pease LR. 1989. Site-directed mutagenesis by overlap extension using the polymerase chain reaction. Gene 77:51–59.
82. Rietsch A, Vallet-Gely I, Dove SL, Mekalanos JJ. 2005. ExsE, a secreted regulator of type III secretion genes in *Pseudomonas aeruginosa*. Proc Natl Acad Sci U S A 102:8006–8011.
83. Kovach ME, Elzer PH, Steven Hill D, Robertson GT, Farris MA, Roop RM, Peterson KM. 1995. Four new derivatives of the broad-host-range cloning vector pBBR1MCS, carrying different antibiotic-resistance cassettes. Gene 166:175–176.
84. Bloemberg G V., O'Toole GA, Lugtenberg BJJ, Kolter R. 1997. Green fluorescent protein as a marker for *Pseudomonas* spp. Appl Environ Microbiol 63:4543–4551.
85. Murashige T, Skoog F. 1962. A Revised Medium for Rapid Growth and Bio Assays with Tobacco Tissue Cultures. Physiol Plant 15:473–497.
86. Haney CH, Samuel BS, Bush J, Ausubel FM. 2015. Associations with rhizosphere bacteria can confer an adaptive advantage to plants. Nat Plants 1.
87. Andrews S. 2010. FastQC: a quality control tool for high throughput sequence data.
88. Patro R, Duggal G, Love MI, Irizarry RA, Kingsford C. 2017. Salmon provides fast and bias-aware quantification of transcript expression. Nat Methods 14:417–419.
89. Love MI, Huber W, Anders S. 2014. Moderated estimation of fold change and dispersion for RNA-seq data with DESeq2. Genome Biol 15:550.
90. Zhu A, Ibrahim JG, Love MI. 2019. Heavy-Tailed prior distributions for sequence count data: Removing the noise and preserving large differences. Bioinformatics 35:2084–2092.
91. Bunis DG, Andrews J, Fragiadakis GK, Burt TD, Sirota M. 2020. dittoSeq: universal user-friendly single-cell and bulk RNA sequencing visualization toolkit. Bioinformatics.
92. Mulet M, Lalucat J, García-Valdés E. 2010. DNA sequence-based analysis of the Pseudomonas species. Environ Microbiol 12:1513–1530.
93. Luo W, Friedman MS, Shedden K, Hankenson KD, Woolf PJ. 2009. GAGE: Generally applicable gene set enrichment for pathway analysis. BMC Bioinformatics 10:161.
94. Grote S. 2020. GOfuncR: Gene ontology enrichment using FUNC. R package 1.10.0.
95. Schroth MN, Cho JJ, Green SK, Kominos SD. 2018. Epidemiology of *Pseudomonas aeruginosa* in agricultural areas. J Med Microbiol 67:1191–1201.
96. Tamayo R, Choudhury B, Septer A, Merighi M, Carlson R, Gunn JS. 2005. Identification of *cptA*, a PmrA-regulated locus required for phosphoethanolamine modification of the *Salmonella enterica* serovar typhimurium lipopolysaccharide core. J Bacteriol 187:3391–3399.
97. Schwartzman JA, Lynch JB, Flores Ramos S, Zhou L, Apicella MA, Yew JY, Ruby EG. 2019. Acidic pH promotes lipopolysaccharide modification and alters colonization in a bacteria–animal mutualism. Mol Microbiol 112:1326–1338.
98. Baetz U, Martinoia E. 2014. Root exudates: the hidden part of plant defense. Trends Plant Sci 19:90–98.
99. Chaparro JM, Badri D V., Bakker MG, Sugiyama A, Manter DK, Vivanco JM. 2013. Root Exudation of Phytochemicals in Arabidopsis Follows Specific Patterns That Are Developmentally Programmed and Correlate with Soil Microbial Functions. PLoS One 8:e55731.
100. Mumm K, Ainsaar K, Kasvandik S, Tenson T, Hõrak R. 2016. Responses of *Pseudomonas putida* to Zinc Excess Determined at the Proteome Level: Pathways

Dependent and Independent of ColRS. J Proteome Res 15:4349–4368.
101. Ueda A, Wood TK. 2009. Connecting quorum sensing, c-di-GMP, pel polysaccharide, and biofilm formation in *Pseudomonas aeruginosa* through tyrosine phosphatase TpbA (PA3885). PLoS Pathog 5:e1000483.
102. Ueda A, Wood TK. 2010. Tyrosine phosphatase TpbA of pseudomonas aeruginosa controls extracellular DNA via cyclic diguanylic acid concentrations. Environ Microbiol Rep 2:449–455.
103. Pu M, Wood TK. 2010. Tyrosine phosphatase TpbA controls rugose colony formation in *Pseudomonas aeruginosa* by dephosphorylating diguanylate cyclase TpbB. Biochem Biophys Res Commun 402:351–355.
104. Schalk IJ, Guillon L. 2013. Pyoverdine biosynthesis and secretion in *Pseudomonas aeruginosa* : implications for metal homeostasis. Environ Microbiol 15:1661–1673.
105. Corbitt J, Yeo JS, Davis I, LeRoux M, Wiggins PA. 2018. Type VI secretion system dynamics reveals a novel secretion mechanism in Pseudomonas aeruginosa. J Bacteriol 200:e00744-17.
106. Singh B, Röhm KH. 2008. Characterization of a *Pseudomonas putida* ABC transporter (AatJMQP) required for acidic amino acid uptake: Biochemical properties and regulation by the Aau two-component system. Microbiology 154:797–809.
107. Maurer LM, Yohannes E, Bondurant SS, Radmacher M, Slonczewski JL. 2005. pH regulates genes for flagellar motility, catabolism, and oxidative stress in *Escherichia coli* K-12. J Bacteriol 187:304–319.
108. Xu Y, Zhao Z, Tong W, Ding Y, Liu B, Shi Y, Wang J, Sun S, Liu M, Wang Y, Qi Q, Xian M, Zhao G. 2020. An acid-tolerance response system protecting exponentially growing *Escherichia coli*. Nat Commun 11:1–13.
109. Séguin V, Courchesne F, Gagnon C, Martin RR, Naftel SJ, Skinner W. 2005. Mineral Weathering in the Rhizosphere of Forested Soils, p. 29–55. *In* Biogeochemistry of Trace Elements in the Rhizosphere. Elsevier.
110. Skirvin RM, Chu MC, Mann ML, Young H, Sullivan J, Fermanian T. 1986. Stability of tissue culture medium pH as a function of autoclaving, time, and cultured plant material. Plant Cell Rep 5:292–294.
111. Hall JL. 2003. Transition metal transporters in plants. J Exp Bot 54:2601–2613.
112. Haichar F el Z, Santaella C, Heulin T, Achouak W. 2014. Root exudates mediated interactions belowground. Soil Biol Biochem 77:69–80.
113. Hegge FT, Hitchen PG, Aas FE, Kristiansen H, Løvold C, Egge-Jacobsen W, Panico M, Leong WY, Bull V, Virji M, Morris HR, Dell A, Koomey M. 2004. Unique modifications with phosphocholine and phosphoethanolamine define alternate antigenic forms of *Neisseria gonorrhoeae* type IV pili. Proc Natl Acad Sci U S A 101:10798–10803.
114. Cullen TW, Trent MS. 2010. A link between the assembly of flagella and lipooligosaccharide of the Gram-negative bacterium *Campylobacter jejuni*. Proc Natl Acad Sci 107:5160–5165.
115. Hagelueken G, Huang H, Clarke BR, Lebl T, Whitfield C, Naismith JH. 2012. Structure of WbdD: A bifunctional kinase and methyltransferase that regulates the chain length of the O antigen in *Escherichia coli* O9a. Mol Microbiol 86:730–742.
116. Trombley MP, Post DMB, Rinker SD, Reinders LM, Fortney KR, Zwickl BW, Janowicz DM, Baye FM, Katz BP, Spinola SM, Bauer ME. 2015. Phosphoethanolamine transferase LptA in *haemophilus ducreyi* modifies lipid a and contributes to human defensin

resistance *in vitro*. PLoS One 10:e0124373.
117. Nairz M, Schroll A, Sonnweber T, Weiss G. 2010. The struggle for iron - a metal at the host-pathogen interface. Cell Microbiol 12:1691–1702.
118. Winterbourn CC. 1995. Toxicity of iron and hydrogen peroxide: the Fenton reaction. Toxicol Lett 82–83:969–974.
119. Pasqua M, Visaggio D, Lo Sciuto A, Genah S, Banin E, Visca P, Imperi F. 2017. Ferric uptake regulator Fur is conditionally essential in *Pseudomonas aeruginosa*. J Bacteriol 199.
120. Arendsen LP, Thakar R, Sultan AH. 2019. The use of copper as an antimicrobial agent in health care, including obstetrics and gynecology. Clin Microbiol Rev 32.
121. Irving H, Williams RJP. 1953. The stability of transition-metal complexes. J Chem Soc 3192–3210.
122. Staudenmaier H, Van Hove B, Yaraghi Z, Braun V. 1989. Nucleotide sequences of the *fecBCDE* genes and locations of the proteins suggest a periplasmic-binding-protein-dependent transport mechanism for iron(III) dicitrate in *Escherichia coli*. J Bacteriol 171:2626–2633.
123. Marshall B, Stintzi A, Gilmour C, Meyer JM, Poole K. 2009. Citrate-mediated iron uptake in *Pseudomonas aeruginosa*: Involvement of the citrate-inducible FecA receptor and the FeoB ferrous iron transporter. Microbiology 155:305–315.
124. Bearson BL, Wilson L, Foster JW. 1998. A low pH-inducible, PhoPQ-dependent acid tolerance response protects *Salmonella typhimurium* against inorganic acid stress. J Bacteriol 180:2409–2417.
125. Prost LR, Daley ME, Le Sage V, Bader MW, Le Moual H, Klevit RE, Miller SI. 2007. Activation of the Bacterial Sensor Kinase PhoQ by Acidic pH. Mol Cell 26:165–174.
126. Batchelor E, Walthers D, Kenney LJ, Goulian M. 2005. The *Escherichia coli* CpxA-CpxR envelope stress response system regulates expression of the porins OmpF and OmpC. J Bacteriol 187:5723–5731.
127. Tack FM, Callewaert OWJJ, Verloo MG. 1996. Metal solubility as a function of pH in a contaminated, dredged sediment affected by oxidation. Environ Pollut 91:199–208.
128. Zan NR, Datta SP, Rattan RK, Dwivedi BS, Meena MC. 2013. Prediction of the solubility of zinc, copper, nickel, cadmium, and lead in metal-contaminated soils. Environ Monit Assess 185:10015–10025.

Appendices – Supplemental Figures and Tables

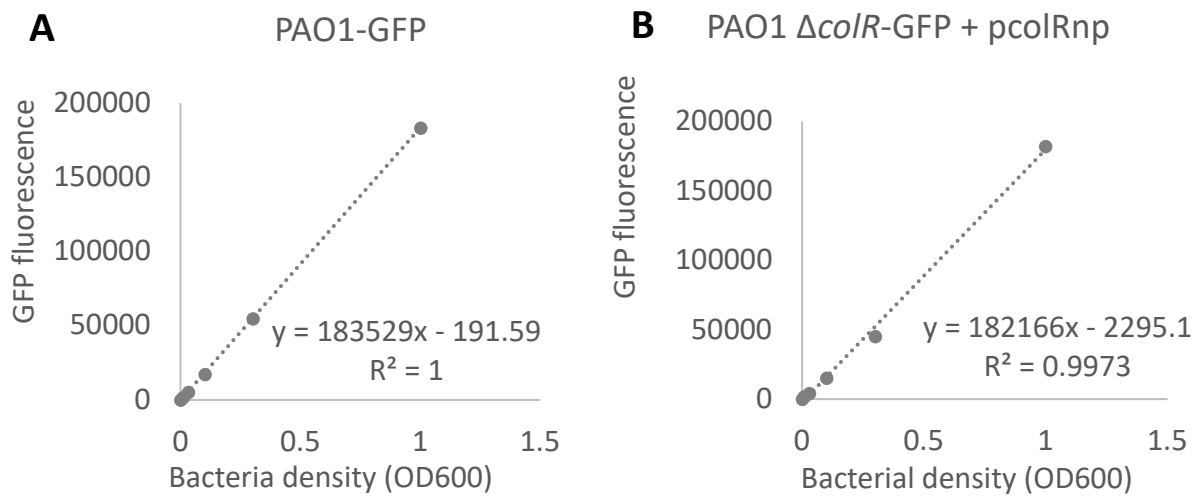

Figure S1. Calibration curves used for the conversion of GFP fluorescence to OD_{600} in the 48-well GFP rhizosphere colonization assay. Overnight cultures of GFP-expressing bacteria were diluted to OD_{600} 0.01, 0.03, 0.1, 0.3, and 1, before aliquoting 300 µl of each dilution in duplicates into 48-well plates and measuring GFP fluorescence. **(A)** The linear trend obtained using PAO1-GFP was used to estimate rhizosphere OD_{600} of all PAO1-derived mutants containing the pSMC21 GFP-expression plasmid. **(B)** The linear trend obtained using PAO1 Δ*colR*-GFP + pcolRnp and used to estimate rhizosphere OD_{600} of PAO1 and PAO1 Δ*colR* containing pSMC21, and either EV or pcolRnp.

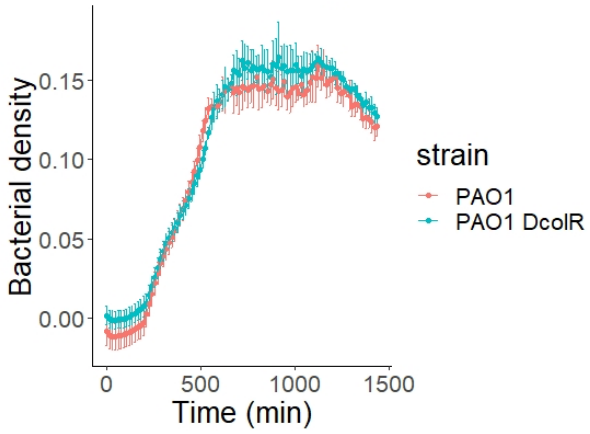

Figure S2. ColR is not required for growth in minimal media. Growth curves of PAO1 and PAO1 Δ*colR* were conducted in M9 minimal media supplemented with 24 mM L-gln in 96-well plates. Plates were incubated at 37˚C, and OD_{600} measurements were taken every 15 min for 24 h. Three replicates were conducted with similar results. A single experimental replicate is shown with averages and standard deviations of 6 technical replicates per time point.

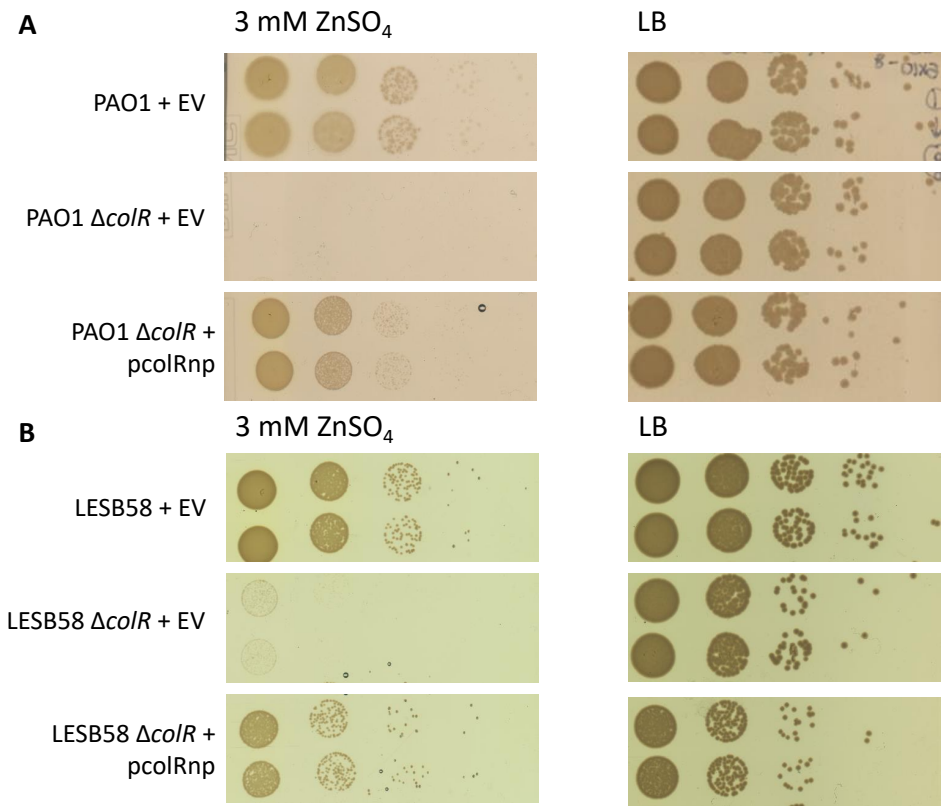

Figure S3. A plasmid encoding *colR* with its native promoter complements zinc tolerance defect of PAO1 Δ*colR* and LESB58 Δ*colR* mutants. Cultures of **(A)** PAO1 or **(B)** LESB58 wildtype and Δ*colR* with empty vector (EV) or the *colR* complementation vector (pcolRnp) were serially diluted and plated in duplicates on LB plates with and without 3 mM $ZnSO_4$. Plates were incubated at 37˚C for 1 (PAO1) or 2 (LESB58) days. Experiments were repeated at least twice, with representative images shown.

Table S1. Strains and plasmids.

Strain or plasmid	Genotype or description	Source
***E. coli* strains**		
DH5α pir	*supE44* Δ*lacU169* (Φ*lacZ*Δ*M15*) *recA1 endA1 hsdR17 thi-1 gyrA96 relA1 zdg-232::Tn10 uidA::pir+*	Lab stock
SM10(λpir)	*thi thr leu tonA lacY supE recA*::RP4-2-*Tc*::Mu Km *λpir*	Lab stock
***P. aeruginosa* strains**		
PAO1 H103	PAO1 subline H103; parental strain of PAO1 mutants and wildtype to the PA two-allele mutant library	(14)
PAO1 Δ*colR*	PAO1 *colR* clean deletion; ColR response regulator mutant	This study
PAO1 Δ*colS*	PAO1 *colS* clean deletion; ColS sensor kinase mutant	This study
PAO1 Δ*eptA*	PAO1 *eptA* clean deletion; pEtN transferase mutant	This study
PAO1 transposon mutants	PA two-allele library generated by the Manoil lab	(76)
LESB58	Liverpool Epidemic strain	(18)
LESB58 Δ*colR*	LESB58 *colR* clean deletion; ColR response regulator mutant	This study
Plasmids		
pEXG2	Gm^R; Vector for *Pseudomonas* spp. allelic exchange	(82)
pSMC21	Cb^R; Ap^R; Km^R; *Ptac-GFPmut2*	(84)
PBBR1MCS-5	Gm^R; Broad host range cloning vector	(83)
pΔ*colR*	pEXG2::Δ*colR*-flanking; allelic exchange vector; used for generating *colR* clean deletion in both PAO1 and LESB58	This study
pΔ*colS*	pEXG2::Δ*colS*-flanking; allelic exchange vector	This study
pΔ*eptA*	pEXG2::Δ*eptA*-flanking; allelic exchange vector	This study
pcolRnp	PBBR1MCS5::$colR_{np}$; *colR* complementation vector with native promoter	This study

Table S2. Primers used for construction of strains and plasmid. For deletion constructs, flanking regions of the gene were amplified and joined using overlap PCR. Primers used for overlap extension PCR are listed in the following order: 1) upstream flanking region outside primer, 2) upstream flanking region inside primer, 3) downstream flanking region inside primer, 4) downstream flanking region outside primer, 5) upstream confirmation primer, 6) downstream confirmation primer. The last two rows are primers used for amplification of *colR* for construction of the pcolRnp complementation plasmid.

Strain	Primer name	Restriction site	Sequence (5' → 3')
PAO1/ LESB58 Δ*colR*	colR_F1	HindIII	AATCGAAGCTTAGCGCGAACAGGACGAATC
	colR_R1	-	CAGCAAGGCCACGGAGAATGGTCCCACTCCTTCGCAGGA
	colR_F2	-	TCCTGCGAAGGAGTGGGACCATTCTCCGTGGCCTTGCTG
	colR_R2	XbaI	AATCGTCTAGACAGCAGTTCGCATGAGGTGG
	colR_seqF	-	AAGTGCGCACCTTGCAGC
	colR_seqR	-	TCGCGCATCTCCTCGGTG
PAO1 Δ*colS*	colS_F1	HindIII	AATCGAAGCTTTTCCTGCGAAGGAGTGGGAC
	colS_R1	-	CGAACCGGCAGCCATGCGGCGAGGCTCTGCTTATACTCC
	colS_F2	-	GGAGTATAAGCAGAGCCTCGCCGCATGGCTGCCGGTTCG
	colS_R2	XbaI	AATCGTCTAGACAGCGGGATGAAATCGAGATGC
	colS_seqF	-	CGAGCGTAGAGCCGGTG
	colS_seqR	-	
PAO1 Δ*eptA*	eptA_F1	XbaI	ATCGATCTAGAGATCACGGTGATCACCGGC
	eptA_R1	-	GAAATAGTCCTTTCGCCGAGTCGTAGGGCACGGATCTTCACTGAC
	eptA_F2	-	TACGACTCGGCGAAAGGACTATTTC
	eptA_R2	BamHI	ATCGAGGATCCATTGCCGGCGTGATAGTGG
	eptA_seqF	-	ACCGATCGGATGGCTGAGGGC
	eptA_seqR	-	CCTCTCCAGCTCGTCCAGTGTCTGC

Plasmid	Primer name	Restriction site	Sequence (5' → 3')
pcolRnp	colRnp_F	XbaI	ACTGTCTAGACTGGGTCATGCGATCTCCAAC
	colRnp_R	HindIII	ACTGAAGCTTCTCTGCTTATACTCCATTCGGCTC

Table S3. Primers used for qRT-PCR.

Gene name	Forward primer sequence (5' → 3')	Reverse primer sequence (5' → 3')
PA0004 (*gyrB*)	GGTGTTCGAGGTGGTGGATA	TGGTGATGCTGATTTCGCTG
PA1972 (*eptA*)	AACGTCATGCAGACCAACCC	CCAAGCAACGCCAGGTAGAC
PA2910 (*mntP*)	GCCTGCACATGATCCACAAC	TCACCGCGAGAATCCAGAAC
PA3310	GCGGTAATGGTAGGCAGCTT	GTCGGGTTGATGAAGTGGGT
PA3223 (*azoR3*)	CATGAACATGGGCCCGGAAT	AAGGGAGGTGTCGGTTTCCA
PA3540 (*algD*)	CCTGTCGCGCTACTACATGC	ATAGGTGAGGGCGCGTACAT
PA3551 (*algA*)	CGCTTCCAGGTCAAGCACAT	CCGGAAACCACGATCCAGTG
PA3885 (*tpbA*)	CATGAGCCCCACCCTCTATC	TGAAGCTGACCACCGTCTTC